



HAL
open science

The impact of biogas digestate typology on nutrient recovery for plant growth: Accessibility indicators for first fertilization prediction

Julie Jimenez, Marco Grigatti, Elisa Boanini, Dominique Patureau, Nicolas Bernet

► To cite this version:

Julie Jimenez, Marco Grigatti, Elisa Boanini, Dominique Patureau, Nicolas Bernet. The impact of biogas digestate typology on nutrient recovery for plant growth: Accessibility indicators for first fertilization prediction. *Waste Management*, 2020, 117, pp.18-31. 10.1016/j.wasman.2020.07.052 . hal-02921497

HAL Id: hal-02921497

<https://hal.inrae.fr/hal-02921497v1>

Submitted on 22 Aug 2022

HAL is a multi-disciplinary open access archive for the deposit and dissemination of scientific research documents, whether they are published or not. The documents may come from teaching and research institutions in France or abroad, or from public or private research centers.

L'archive ouverte pluridisciplinaire **HAL**, est destinée au dépôt et à la diffusion de documents scientifiques de niveau recherche, publiés ou non, émanant des établissements d'enseignement et de recherche français ou étrangers, des laboratoires publics ou privés.



Distributed under a Creative Commons Attribution - NonCommercial 4.0 International License

1 **The impact of biogas digestate typology on nutrient recovery for plant growth: accessibility**
2 **indicators for first fertilization prediction**

3 Julie Jimenez¹, Marco Grigatti², Elisa Boanini³, Dominique Patureau¹, Nicolas Bernet¹

4 ¹LBE, INRAE, Univ Montpellier, 102 Avenue des Etangs, Narbonne, F-11100, France

5 ² Department of Agricultural and Food Sciences, Alma Mater Studiorum, University of Bologna, Viale
6 G. Fanin, 40, 40127 Bologna, Italy

7 ³ Department of Chemistry “Giacomo Ciamician”, Alma Mater Studiorum – University of Bologna,
8 Via Selmi 2, 40126 Bologna, Italy

9 E-mail: julie.jimenez@ inrae.fr

10 **Abstract**

11 In recent years, anaerobic digestion of organic waste (OW) is rapidly appearing as a winning waste
12 management strategy by producing energy and anaerobic digestates that can be used as fertilizers in
13 agricultural soils. In this context, the management of the OW treatment process to maximize agro-
14 system sustainability satisfying the crop nutrient demands represents the main goal. To investigate
15 these traits, two protocols to assess the plant availability of digestate nitrogen (N) and phosphorus (P)
16 were evaluated. With this aim, the N and P availability was determined on 8 digestates and 2 types of
17 digestate-based compost from different OW via sequential chemical extractions (SCE). In addition, the
18 digestates were tested in soil incubations and in plant pot tests with Italian ryegrass and compared with
19 chemical fertilizer and a non-amended control soil. The N extracted from digestates via SCE was
20 related to soil N mineralization and plant N recovery. The C: N ratio had negative impact on
21 mineralized N and its recovery in shoots ($\text{Shoots}_N = -0.0085 \times \frac{C}{N} + 0.1782$, $r^2=0.67$), whereas water
22 extractable mineral N was positively related to the root N apparent recovery fraction (N-ARF) with
23 ($\text{Roots}_N = 5E^{-5} \times N_{\text{solublemin}} + 0.0138$, $r^2=0.53$). The shoot P-ARF was positively correlated with the
24 inorganic water extractable fraction of P ($\text{Shoots}_P = 0.1153 \times H_2O - P_i - 0.2777 \times H_2O - P_o +$
25 0.0249 , $r^2=0.71$) whereas the root P-ARF was positively correlated with the less accessible fractions

26 $(\text{Roots}_p = 0.0955 \times \text{NaHCO}_3\text{P}_0 + 0.0955 \times \text{NaOH P}_0 - 0.0584 \times \text{NaHCO}_3\text{P}_1 + 0.0128, r^2=0.8641)$.

27 Feedstock digestate typology impacted the N and P recovery results leading to a better description of
28 the typology properties and a first nutrients ARF prediction.

29 **Key words** digestates, typology, fertilizers, characterization indicators, nutrient recovery

30

31 **1. Introduction**

32 An increasing interest exists in improving the soil quality following the utilization of organic wastes
33 (OW) within the environmentally friendly bio-refinery approach (Albuquerque et al., 2012; Gissén et
34 al., 2014). In this respect, anaerobic digestion is a major building block in the circular bioeconomy.
35 Furthermore, both energy (ie. biomethane) and organic fertilizers (ie. digestate) replacing the chemical
36 fertilizers provided to crops can be recovered from anaerobic digestion of OW. From an agronomic
37 and economic point of view, digestate use as a fertilizer can be considered not only as a supplement
38 for traditional organic fertilizers (i.e. slurry) but also as an alternative fertilizer, which under certain
39 soil conditions, is more effective than using NPK fertilizer (Barlog et al., 2019). Indeed, anaerobic
40 digestion is reported as a suitable treatment to easily recover P and N fertilizers from digestate
41 (Mazzini et al., 2020). This is due to organic matter and free organic nutrients biodegraded into
42 mineral forms. However, agricultural reuse of treated OW as soil fertilizers is limited by
43 environmental constraints related to the quality of organic matter, nutrient availability and safety
44 issues. Furthermore, the chemical composition of digestate depends on the nature of feedstock and
45 digestion process (Albuquerque et al., 2012, Guilayn et al., 2019, Barlog et al., 2019). Indeed, a
46 statistical classification of 91 digestates based on their agronomic quality (i.e. C, N, P, total solids,
47 organic matter) was applied on a large range of raw digestates by (Guilayn et al., 2019) and revealed 6
48 groups of different digestate typology. By analyzing the obtained digestates groups, two criteria
49 impacted the classification: the TS concentration of the digestates associated with dry or wet anaerobic
50 digestion process and the feedstock type, as following: liquid fibrous feedstock (crop residues silage,
51 cattle slurry), liquid sewage sludge, liquid pig slurry, slurries co-digested with silage and green wastes

52 (dry anaerobic digestion), municipal solid wastes (dry anaerobic digestion) and fibrous feedstock (dry
53 anaerobic digestion of cattle manure and green waste). In this framework, mineral N can be readily
54 available for crops but can be temporarily immobilized by microbial biomass during OW
55 mineralization in soil (Lashermes et al., 2010). Therefore, it is important to know the OW
56 mineralization N kinetics to optimize the N supply synchronisation with plant requirement in
57 agricultural systems.

58 In this context, to better control and manage the quality of digestates, a better knowledge of the
59 accessibility and availability of nutrients and organic matter would improve the fertilizing potential of
60 these products. According to Möller et al. (2012), an accurate characterization of digestate nutrient
61 content and organic matter (OM) composition, combined with experiments to assess the N
62 mineralization and N immobilization processes after field spreading, would be essential for a better
63 characterization of the driving factors driving N turnover in the soil.

64 Total content of nutrients in OW hardly predicts their fertilizer potential. Ahmad et al. (2018) reported
65 more than 80% of applied P is rapidly immobilized being unavailable for plant following
66 adsorption/precipitation processes or conversion into organic form. To gain a better insight on this
67 issue, many authors proposed to characterize the available P via P fractionation. He et al. (2010)
68 reported that bioavailability of applied P depends on the presence of specific P forms and that labile P
69 includes the sum of inorganic and organic P from H₂O and NaHCO₃ extracted fractions. In this regard,
70 Grigatti et al. (2015; 2017; 2019), performed a dedicated SCE on digestates and composts in order to
71 measure the phosphorous potentially available for plants. The authors found good correlations
72 between the water- and the sodium bicarbonate-extractable P from composts with short- and medium-
73 term plant P uptake.

74 Lashermes et al. (2010) proposed an OW classification based on their chemical characteristics to
75 predict N availability. However, only 2% of the 273 OW studied came from similar typology of
76 digestates coming from fibrous feedstock anaerobic digestion with low N availability (i.e. digestates
77 was classified in a group with initial N concentration under 65 g kg⁻¹ and C: N ratio around 15).
78 However, according to Guilayn et al. (2019), the N content from digestates varies from 20 g kg⁻¹ to
79 175 g kg⁻¹ and C: N ratio varies from 2 to more than 30. It would be interesting to complete the

80 Lashermes study with different typologies of digestate to classify their fertilizer potential. To do that,
81 the first step would be to evaluate the impact of digestate typology on plant growth. Recently, a
82 methodology proposed for organic matter characterization has been applied to a large range of OW in
83 order to predict both bio-availability and complexity/biodegradability of the organic matter (Jimenez et
84 al., 2015). This technique has been successfully used for OM biodegradation kinetics modelling
85 (anaerobic digestion, compost, soil) (Jimenez et al., 2017) and for organic N dynamics in anaerobic
86 digestion (Bareha et al., 2018; 2019). The basic idea was to find a consistent characterization method
87 in order to describe the bioprocess kinetics and to model the whole treatment chain in terms of organic
88 carbon fate, e.g. anaerobic digestion, compost and organic matter fate in soil. The methodology used is
89 based on SCE to simulate organic matter bioaccessibility for microorganisms combined with three-
90 dimensional fluorescence spectroscopy to analyze the organic matter complexity. The challenge is
91 now to transfer this technique to the characterization of nitrogen accessibility in order to predict its
92 fate after land-spreading and its availability for plant growth.

93 Apart from the previously mentioned studies, there is no literature information on the development of
94 indicators for both N and P plant availability from digestates. This is the reason this study aimed to
95 propose indicators based on chemical extractions and characterization for N and P.

96 In this light, the objectives of this work were to determine the plant-available N and P fractions based
97 on characterization of the accessibility study in order to: (i) assess the impact of typology of OW on
98 the nutrient availability, and (ii) use these indicators to predict plant's nutrients recovery. This study,
99 focussed on a wide range of anaerobic digestates from many types of OW. The results could be used
100 for rapid diagnostic of the (N, P) fertilization potential of a digestate.

101 **2. Materials and methods**

102 **2.1. Organic waste**

103 In order to ensure a representative survey, the anaerobic digestates used in this work were selected on
104 the basis of the results reported by Guilayn et al. (2019). The typology developed by (Guilayn et al.,
105 2019) was used to select the digestate samples out of a large panel of digestates. For this study, 6 main

106 groups were selected from a statistical study applied to the agronomic characteristics: sewage sludge,
107 municipal waste, cow manure (dry -anaerobic digestion), pig manure (liquid anaerobic digestion),
108 centralised (co-digestion), and crop residues. Table 1 presents the samples used with the type of OW
109 used as feedstock and the conditions of the anaerobic digestion process. Post-treated digestates
110 through phase separation (solid or liquid) and composting were also added. Indeed, phase separation is
111 the most classical digestate post-treatment (Alburquerque et al., 2012), leading to two products of
112 different quality (i.e. solid phase as soil amendment and liquid phase as fertilizer). Besides, two
113 digestate-based types of compost (FFMSW_2 and Sludge_2) were used since composting is widely
114 adopted treatment for the solid phase of urban OW digestate to meet the European fertilizing
115 regulation parameters (European Parliament and Council of the European Union, 2016). The organic
116 waste samples were freeze-dried and ground (\varnothing 1mm), in order to reduce the particle size effect in the
117 soil incubations and plant growth experiments.

118 **2.2. Analytical measurements**

119 Freeze-dried ground samples were further ball milled and analysed for the main physico-chemical
120 parameters. The moisture was determined at $105 \pm 2^\circ\text{C}$ until constant weight (24-48h), the volatile
121 solid (VS) was determined on the total solids (TS) at 550°C for 4 h. The total carbon (TC) and total
122 nitrogen (TN) were determined via an elemental analyser (FlashSmart, Thermo Fisher Scientific). The
123 total nutrient and trace elements were determined by ICP (Inductively Coupled Plasma-OES, Spectro
124 Arcos, Ametek) on ≈ 250 mg of samples after microwave assisted digestion with 65% HNO_3 + 37%
125 HCl. All the analyses were done in duplicates.

126 Based on Jimenez et al. (2015), the sequential chemical extractions of organic matter were applied on
127 the freeze-dried and grounded samples (0.5 g). An orbital shaker was used for the extractions steps as
128 following described: 30 mL of 0.01M CaCl_2 (twice, 1h, 30°C , 300 rpm) ; 0.01M (NaOH+NaCl) (4
129 times, 15 min, 30°C , 300 rpm); 0.1M HCl (once, 1h, 30°C , 300 rpm), 0.1M NaOH (4 times, 1h, 30°C ,
130 300 rpm) and 72% H_2SO_4 (twice, 3h, 30°C , 300 rpm). The fractions names are respectively:
131 Soluble extracted from Particulate Organic Matter (SPOM), Readily Extractible Organic Matter
132 (REOM), Slowly Extractible Organic Matter (SEOM) and Poorly Extractible Organic Matter

133 (PEOM). The not extracted fraction is called Non Extractible Organic Matter (NEOM). Each
 134 extraction was done in two replicates, centrifuged and the supernatant collected and filtered. The
 135 recovered pellets were submitted to the subsequent extraction. Ammonium and total nitrogen were
 136 measured in the supernatants using HachLange® kits based on colorimetry methods (LCK 303, 2-47
 137 mg N L⁻¹, and LCK 238, 5-40 mg L⁻¹ respectively).
 138 The organic products were submitted to P fractionation via SCE according to the method of Dou et al.
 139 (2000). Freeze-dried and ball-milled products were extracted for 24 h with deionized water (H₂O) in
 140 an end-over-end shaker, and then centrifuged. The supernatants were passed through a Whatman #42
 141 filter, and the recovered pellets were extracted with 0.5 M NaHCO₃ (pH 8.5) for 24 h. The same
 142 procedure was repeated with 0.1N NaOH and 1N HCl. The residual pellets were treated with a mixture
 143 of 96% H₂SO₄ and 30% H₂O₂ via hot acid digestion at 360 °C. Inorganic P (P_i) in the extracts was
 144 determined via the molybdenum blue method of Murphy and Riley (1962). The P recovered in each
 145 fraction [water extractable P (H₂O-P), bicarbonate extractable P (NaHCO₃-P), alkali extractable P
 146 (NaOH-P), acid extractable P (HCl-P), Residual-P] was calculated as follows:

$$147 \quad P_{i \text{ fraction } x} (\%) = \frac{P_{i \text{ fraction } x}}{P_{\text{tot OW}}} \times 100 \quad \text{Equation 1}$$

148 where $P_{i \text{ fraction } x}$ is the inorganic P determined in each fraction (H₂O, NaHCO₃, NaOH, HCl, Residual),
 149 and $P_{\text{tot OW}}$ is the total-P determined in the different organic waste via ICP after microwave-assisted
 150 acid digestion.

151 The total recovery was calculated as the sum of all fractions (H₂O-P + NaHCO₃-P + NaOH-P + HCl-P
 152 + Residual-P) by using the Equation2:

$$153 \quad \text{Tot } P_{\text{recovery}} (\%) = \frac{\sum_{\text{H2O}}^{\text{Residual}} P_{i \text{ fraction } x}}{P_{\text{tot OW}}} \times 100 \quad \text{Equation 2}$$

154 where $\sum_{\text{H2O}}^{\text{Residual}} P_{i \text{ fraction } x}$ represents the sum of the single P recovery values (P_i) in each fraction (H₂O-P +
 155 NaHCO₃-P + NaOH-P + HCl-P + Residual-P), and $P_{\text{tot OW}}$ is the total P determined in the different
 156 products via ICP after microwave-assisted acid digestion. Organic P was calculated as the difference
 157 between P_{tot} and P_i in the first four fractions.

158 According to He et al. (2010), H₂O-P, NaHCO₃-P, NaOH-P and HCl-P are respectively water-soluble,
159 bioavailable, potential bioavailable (Fe/Al bound) and Ca-bound P.

160

161 **2.3. X-ray diffraction**

162 Samples submitted to X-ray diffraction analysis were carefully ground and placed in a flat stage
163 sample holder. Data were collected by means of a PANalytical X'Pert PRO powder diffractometer
164 equipped with a fast X'Celerator detector. Cu K α radiation was used (40 mA, 40 kV). The 2 θ range
165 was from 5° to 60° with a step size of 0.1° and time/step of 100 s. Data were processed for phase
166 identification using a HighScore Plus software package (PANalytical).

167

168 **2.4. Soil incubation**

169 **2.4.1. Soil**

170 The soil used for the incubation and pot trial was collected from the top layer in a field in the Po
171 Valley (Bologna, Italy). This soil showed the following characteristics: pH (H₂O 1:2.5), 7.90; particle-
172 size distribution; 184 mg kg⁻¹, sand, 425 mg kg⁻¹, silt, 391 mg kg⁻¹ clay; total CaCO₃, 85 g kg⁻¹; total
173 organic carbon (TOC), 10.2 g kg⁻¹ ; total Kjeldahl nitrogen (TKN), 1.60 g kg⁻¹; C:N, 8.3; exchangeable
174 K, 330 mg kg⁻¹ as K₂O, CEC 27.2 meq. 100 g⁻¹. The total (extractable in aqua regia + HF) Al, Fe and P
175 were 35661, 22224 and 808 mg kg⁻¹ respectively. The NH₄-oxalate (pH 3) extractable Al and Fe were
176 764 and 2158 mg kg⁻¹ respectively, while the Na dithionite-citrate extractable Al and Fe were 281 and
177 2462 mg kg⁻¹ respectively.

178 **2.4.2. Incubation tests**

179 Soil incubation was conducted in 500 ml plastic vessels with perforated plastic cap, on 250 g of soil
180 (TS basis). The soil was rewetted at 60 % of the water holding capacity (WHC) and pre-incubated for
181 4 weeks at 25 °C in the dark. Water content was kept at 60% of WHC by weighing the vessels every
182 2-3 days and by adjusting with water drops if needed. After this period, the organic products (i.e.
183 digestates) were added to the soil at 170 kg N ha⁻¹, defined as the maximum N load per year

184 authorized by the European Nitrates Directive (1991) and accurately mixed by hand. Chemical
 185 references used as positive control (Ctrl⁺) were added by distributing N (as NH₄NO₃) at the same
 186 concentration of 170 kg N ha⁻¹, and in addition P and K were added at 117 and 147 kg ha⁻¹ (as
 187 KH₂PO₄). On the basis of N loading the P added to the soil with the different organic product was on
 188 average 20.45 +/- 2.5 mg P kg soil⁻¹. Calculation of the amount of digestate mass added is described
 189 by the Equations 3 to 5 considering 0.3 m of soil depth (d) and a bulk density of 1.33 g/cm³ for 1 ha of
 190 soil.

$$191 \text{ dosis} \left(\frac{\text{mgN}}{\text{kg soil}} \right) = \frac{\text{dosis} \left(\frac{\text{mgN}}{\text{ha}} \right)}{\text{area}_{1 \text{ ha}} \times d} = \frac{170 \times 10^6}{10^4 \times 0.3 \times 1.33 \times 10^3} = 44 \text{ mgN} \cdot \text{kg}^{-1} \quad \text{Equation 3}$$

$$192 \text{ dosis} \left(\frac{\text{gN}}{\text{kg soil}} \right) = \frac{m_{\text{digestate}} \times N_{\text{digestate}} \times \text{TS}_{\text{digestate}}}{m_{\text{soil}}} \quad \text{Equation 4}$$

193 From the Equation 4, digestate amount is calculated as:

$$194 m_{\text{digestate}} = \frac{\text{dosis} \times m_{\text{soil}}}{N_{\text{digestate}} \times \text{TS}_{\text{digestate}}} \quad \text{Equation 5}$$

195 $m_{\text{digestate}}$ is the digestate mass (kg)

196 $N_{\text{digestate}}$ is the N concentration of the digestate (gN.kgTS⁻¹)

197 $\text{TS}_{\text{digestate}}$ is the Total solids content of the digestate (% of fresh matter)

198 m_{soil} is the considered soil mass in the test (kg)

199 Three replicates for each treatment were assessed in a completely randomized block design, in
 200 addition to an unfertilized treatment control (Ctrl⁻). Two parallel soil sampling series were done to
 201 follow the P and N evolution during incubation. Olsen-P, was determined according to Watanabe and
 202 Olsen (1965) at days: 0, 14, 28, 56, 84. The Olsen-P data were used to calculate the relative percentage
 203 extractable (RPE) P, used to normalise the P extractability for each treatment relative to Olsen-P
 204 obtained for Ctrl⁺ (Grigatti et al., 2019). The mineral N course in soil was assessed by extracting soil
 205 samples (1g TS basis) at days 0, 14, 28, 56 and 84 with 1M KCl for 30 min on an end-over-and end
 206 shaker. The solution was filtered over a Whatman #42 filter and ammonium and nitrates were

207 determined using Hach Lange® kits (LCK 304, 0.015-2 mg N.L⁻¹ and LCK 339, 0.23-13.5 mg N L⁻¹
208 respectively).

209 **2.5. Plant pot trials**

210 Based on Grigatti et al. (2014 ; 2015), the digestate samples were added to the ground soil at 170 mg
211 N kg⁻¹ and thoroughly mixed by hand in 2 liter plastic pots (ø 140 mm × h 150 mm). These were filled
212 with 1 liter of inert material (agricultural light expanded clay), and 1 kg of each different treated soil in
213 3 replicates. Pots were seeded with 0.8 g of seeds of Italian ryegrass (*Lolium multiflorum* subsp.
214 *Italicum*), cv. Sprint, covered with a thin layer of sand to prevent drying, watered and placed in a
215 growth chamber at 16-18 h day-night photoperiod at 13–23 °C (±3 °C) day-night temperature, the light
216 was ensured by 6 Philips Master Tld 58 W-840 tubes. Besides the organic products, an unfertilized
217 control (Ctrl⁻), and a chemical reference (at the same rate used for soil incubation) was added (Ctrl⁺).
218 The same treatments and dosis performed in soil incubation test were applied. The use of fast growing
219 species as ryegrass in controlled conditions (moisture; temperature; light) leads to a multiple harvest
220 approach giving the opportunity to the best description of apparent N and P utilization kinetics in the
221 time frame of a growing season (Gunnarson et al., 2010; Schiemenz et al., 2010 ; Tampio et al., 2016).
222 After emergence, plants were regularly watered with tap water to keep soil at 60 % Water Holding
223 Capacity (WHC). At each harvest, ryegrass plants were cut 2 cm above ground and collected 3 times:
224 at 28, 56 and 84 days after sowing. The plant biomass was then dried in a forced air oven at 60 °C for
225 3 days and weighed, to determine dry weight (DW) per pot. Dry biomass was also ball-milled for
226 subsequent analysis. At the last harvest, the roots were divided from the soil with a combined water-
227 sieving separation, and the root biomass was then dried as above, weighed and milled. On plant tissue
228 (shoots and roots), the total P content was determined by means of ICP after (HNO₃, H₂O₂,)
229 microwave assisted digestion. The total N content was determined by elementar analysis as the OW
230 samples. Apparent plant N and P utilization efficiency was calculated on the basis of the Apparent
231 Recovery Fraction (ARF) approach (Gunnarson et al., 2010), according to the Equation 6:

$$232 \text{ ARF}_X (\%) = \frac{\sum_{i=1}^3 \text{X uptake treatment}_{ti} - i \text{X uptake ctrl}^{-}_{ti}}{\text{X added}} \quad \text{Equation 6}$$

233 in which X uptake treatment (t_n) is the total nitrogen or phosphorus uptake (mg pot^{-1}) of a fertilizer
234 treatment at time t ($i = \text{cut 1-3.}$); X uptake ctrl_i is the total nitrogen or phosphorus uptake (mg pot^{-1}) of
235 the unfertilized control at time t ($i = \text{cut 1-3.}$); X added is the total nitrogen or phosphorus added to the
236 pot (mg pot^{-1}).

237 Chemical nutrient equivalent coefficient k_{eq} is defined as the equivalent chemical nutrient dosis (i.e.
238 positive control) percentage needed to reach similar crop yield and is calculated according the
239 Equation 7.

$$240 \quad k_{eq}X = \frac{ARF_X}{ARF_{Ctrl+}} \quad \text{Equation 7}$$

241 **2.6. Statistical analysis**

242 All the data from the plant growth experiment were analyzed by means of Kruskal-Wallis non
243 parametric test. Principal Component Analysis (PCA) and Hierarchical Clustering Analysis (HCA)
244 were also performed on all the data using FactomineR package from the R software. Partial Least
245 Square Regression (PLSR) was performed for variables prediction using the SIMCA® software. For
246 PCA analysis, data from Grigatti et al. (2019) were included as far as similar experiments were done
247 on P speciation and plant pot tests. The three samples were D1, D2 and BD, which are respectively
248 digestate from thermophilic wastewater sludge digestion, digestate from mesophilic winery sludge
249 treatment and digestate from mesophilic bovine slurry and energy crops treatment. Table 1 presents
250 these samples, the conditions of the anaerobic digestion process and the associated feedstocks.

251 **3. Results and discussion**

252 **3.1. Digestates characterization**

253 The main physico-chemical characteristics of the studied digestates are reported in the Table 2. A high
254 variability of the parameters analysed was apparent. Indeed, organic matter ranged between 40 and
255 and 90% (TS basis), the TKN varied between 15 and 45 g kg^{-1} while P ranged between 4 and 20 g kg^{-1} .
256 The most N-rich samples (44-48 g kg^{-1}) were the liquid phase of the centralised digestate (Centr_2),
257 the pig manure digestate (Agri_2) and the sludge digestates (Sludge_1, D1 and D2). The poorest

258 samples were the digestates of FFMSW and its compost (between 15 and 17 g N kg⁻¹). The richest P
259 samples were the sludge digestate (Sludge_1) and its compost (Sludge_2), along with the solid phase
260 of the centralised digestate (Centr_1) and digestate D2 (sludge from winery processing) with a P
261 content ranging between 18 and 20 g kg⁻¹. The FFMSW_1 digestate and its compost FFMSW_2
262 besides the silage straw digestate (Agri_3) were the poorest P samples (4 g P kg⁻¹). PCA and HCA
263 analyses were performed on the samples characteristics for a whole sight of the digestates profiles thus
264 allowing the comparison with the typology of Guilayn et al. (2019). The results are presented in the
265 Supplementary Material (Figure A.1). The PCA was applied on nine parameters (i.e from TS to K in
266 Table 2). The first two components recovered $\approx 80\%$ variance. The first component (PC1) was mainly
267 related to the TS, negatively related to OM and K.

268 PC1 clustered dried (i.e. FFMSW_1, composts Sludge_2 and FFMSW_2) and liquid AD digestates
269 (i.e. all the others). The second component (PC2) was formed by P, which was negatively related to
270 the C: N ratio related to fibrous composition. The sludge digestate samples were associated with P
271 concentration variable whereas Agri_3 (wheat straw digestate) was mainly associated to C: N ratio
272 variable. Furthermore, Sludge_1 and 2 were the samples containing the highest metals concentrations
273 (Fe, Al, Pb, Cu, Mn, Mo, and Cd).

274 These results were in agreement with the raw digestate typology found by Guilayn et al. (2019).
275 Indeed, Agri_1 and Agri_3 characteristics were in agreement with the characteristics associated to the
276 fibrous feedstock digestate group after dried digestion (i.e. cattle manure and crop residues). Agri_2
277 characteristics were consistent with those of the pig slurry digestate group from the typology.

278 Sludge_1 characteristics were consistent with those of the sludge digestate group and FFMSW_1
279 characteristics fit with the municipal solid wastes digestate group characteristics. BW_1
280 characteristics were mainly close to the biowaste and municipal solids waste digestate composition
281 after dry digestion. However, NH₄ concentration and NH₄: TN ratio had similar values than the
282 manure co-digestion (i.e. NH₄: TN ratio > 70%). This is probably due to the high ratio of agro-
283 industrial waste in the feedstock used in addition of biowastes. Only digestate from the wet digestion
284 of fibrous substrate was not taken into account (silage) in this study. Composts Sludge_2 and

285 FFMSW_2 and Centr_1 and 2 obtained after phase separation were not compared with the typology as
286 they were not raw digestates.

287 Attention should be paid to the results for TKN and N-NH⁺₄ concentration obtained by the raw sample
288 analysis and to the freeze-dried sample extraction analysis. Regarding some digestates, highly
289 significant positive differences were obtained between raw and freeze-dried samples analyses (from
290 40% for Centr_2 to 61% for Agri_2 of TKN loss). This result was due to ammonia volatilization
291 during freeze-drying operation. The loss of ammonia could have an impact on soil incubation and
292 plant N recovery results. Considering the 8 others digestates, no significant differences appeared and a
293 linear relation was obtained between raw sample analysis and freeze-dried analysis (i.e. $TKN_{raw} =$
294 $0.9443 \cdot TKN_{freeze-dried}$, $R^2 = 0.8832$). Furthermore, the N typology of Agri_2 became similar as
295 Agri_1 and 3 (fibrous feedstock involving manures). NH₄: TN ratio evolved from 76% to 39%. This
296 ratio decreased also for Centr_2 from 46% to 9% after freeze-drying. Consequently, Agri_2 and
297 Centr_2 results were used in statistical tests by using the freeze-dried analysis. N-ARF recovery will
298 be discussed accordingly. However, concerning liquid digestates with high ammonia content as pig
299 slurry digestates, the best option would be to perform soil incubation and plant pot trials with fresh
300 matter as Rigsby et al. (2013), de la Fuente et al. (2013). A higher mass of soil would be required to
301 maintain the soil WHC with the liquid digestate moisture, according Equation 5.

302 This first characterization approach showed that the digestates selected were representative of a large
303 range of digestates (i.e. municipal waste, sludge, manure, crop residue, bio-wastes, centralised).

304 **3.1.1. X-ray powder diffraction**

305 The X-ray powder diffraction has been widely use for the study of the crystalline P species in anaerobic
306 digestate and compost (Li et al., 2019; Grigatti et al., 2017; 2019). In this light the XRD profiles from the
307 tested products can give a valuable insight to their P extractability. The XRD patterns from the digestates
308 are presented in Figure 1. The XRD patterns of samples Agri_1, Agri_2 and Agri_3 were similar
309 showing the presence of crystalline inorganic phases, namely quartz (PDF no. 01-087-2096), calcite
310 (PDF no. 01-085-1108) and sylvine (KCl, PDF no. PDF no.41-1476).

311 However, these three samples differed significantly in their amorphous phase content, which was
312 definitively higher in Agri_3, followed by Agri_1, whereas sample Agri_2 was mostly constituted of
313 crystalline material. Furthermore, Agri_2 presents also struvite peaks (PDF no. 15-0762), that could be
314 detected on account of the higher crystallinity of this sample. Amongst the analyzed samples, Sludge_1
315 was the most crystalline one, with no significant presence of amorphous material. The Sludge_1 pattern
316 showed the presence of calcite and quartz as main constituting phases, together with a low amount of
317 vivianite ($\text{Fe}_3(\text{PO}_4)_2(\text{H}_2\text{O})_8$, PDF no. 01-075-1186). Li et al. (2018) found also that quartz was one of the
318 major phases for sewage sludge. Sludge_2 was somewhat similar to Sludge_1, but less crystalline so that
319 only calcite and quartz were detected (in this case quartz is more abundant than calcite). FFMSW_1 and
320 FFMSW_2 were very similar both regarding the amount of amorphous phase which is present together
321 with the fine crystalline fraction of the materials. Regarding the qualitative detection of crystalline
322 phases, it was possible to identify quartz (the most abundant), calcite, together with low amounts of
323 kaolinite ($\text{Al}_2(\text{Si}_2\text{O}_5)(\text{OH})_4$, PDF no.01-080-0885) and sylvite. BW_1, Centr_1 and Centr_2 patterns all
324 displayed the presence of quartz, calcite and struvite as crystalline components, but significantly differed
325 for the amount of amorphous material that was relatively low in Centr_2, and higher and similar in
326 BW_1 and Centr_1. The relationship between the XRD outcomes and the P extractability are discussed
327 in the following section.

328 **3.1.2. Sequential chemical extractions of Nitrogen and Phosphorous**

329 The N fractionation protocol used in this work was developed by Jimenez et al. (2015), and has been
330 validated to describe OM and N evolution during biological degradation processes (Jimenez et al.,
331 2017 and Bareha et al., 2018). The P fractionation has been adapted from Hedley et al. (1982), using
332 methodology by Grigatti et al. (2015, 2017, and 2019). These authors showed the link between labile-
333 P from organic waste samples and the plant P-uptake. The N and P speciations have been assessed
334 applying both fractionation protocols to the selected digestates (Figure 2 a and b respectively). The
335 results showed that the digestates performed different N and P speciations. This was related to the
336 digestate typology and the nature of the feedstock for anaerobic digestion, according to Guilayn et al.

337 (2019). The observed variability in N and P speciation showed the significant effect of the feedstock on
338 the tests discussed in section 3.2. In the study of N accessibility (Figure 2 a), mineral nitrogen was
339 assessed in the water extractable fraction SPOM. The non-extractable organic nitrogen varied between
340 25 and 48% except for Agri_3 with only 5% N in the NEOM fraction.

341 HCA was applied on the N speciation data (not shown). Four groups were found, ordered by N
342 accessibility basis as follows: (i) Group 1: High NH₄-N SPOM samples: Centr_1 and BW_1. This
343 result is consistent since these samples had poor TS; (ii) Group 2: High organic SPOM and REOM:
344 Agri_2 and Sludge_1. SPOM and REOM are mainly composed of accessible and readily extractable
345 proteins; (iii) Group 3: High organic SEOM: Agri_3. SEOM is mainly composed of complex proteins
346 and humic-like substances; (iv) Group 4: High PEOM organic N content samples: Agri_1, FFMSW_1,
347 Centr_2, FFMSW_2 and Sludge_2. PEOM extraction targets holocellulose-like compounds found in
348 fibrous digestates as Agri_1, FFMSW_1 and 2. Phase separation concentrates OM and fibers in the
349 solid phase (Guilayn et al., 2019) as Centr_2. Finally, the compost Sludge_2 was also clustered in this
350 group because of its co-composting with green wastes.

351 P was extracted in each fraction as reported in Figure 2 b. Phosphorus fractionation showed that
352 inorganic P content was higher than organic P in all the fractions, as reported in the studies of Grigatti et
353 al. (2015, 2017 and 2019) on digestates and composts, and as observed by He et al. (2010) on poultry
354 litter and dried wastewater sludge. Mazzini et al. (2020) showed that 78 to 93% of TP was inorganic
355 following the SCE from six types of animal slurries digestates. The authors showed relevant NaOH (5-
356 43% of organic P) and HCl (2-25% of organic P) extractable organic P, relating this to inorganic P
357 microbial immobilization during anaerobic digestion for microorganism growth. Indeed, soluble
358 inorganic P would be transformed into organic P compounds such as phosphates monoesters or DNA.
359 This biological organic-P may be rapidly mineralized once in soil (He et al., 2010). In this context,
360 NaOH and H₂O were the most organic-P rich fractions from the samples investigated in this work.
361 Furthermore, Agri_1, 2 and 3, and FFMSW_1 mainly showed NaOH extractable organic P. Agri_3
362 contained the highest organic P content (\approx 40%), and 1.5 to 4- folds higher than other samples. In water
363 Agri_2 and 3 showed 60% of organic P, higher than BD (49%).

364 The results obtained by He et al. (2010) on poultry litter showed that a large part of organic P was in the
365 NaOH fraction and was mainly related to phytate-like. Mazzini et al. (2020) showed similar results on
366 crop residues digestates. The authors showed also that organic P were mainly extracted in NaOH fraction
367 of 6 agro-wastes digestates as shown by Agri_1 and 3. Organic P was observed in HCl fraction from
368 Sludge_1 and 2 in this study. He et al. (2010), observed also organic P in HCl fractions related to non-
369 hydrolysable fractions in the dried wastewater sludge. The NaHCO₃ and the HCl fractions showed to be
370 the most inorganic P rich fractions from the samples tested in this work thus fitting to available P and Ca-
371 bounded P. The labile-P fraction (H₂O + NaHCO₃) was found at the highest level in the agricultural
372 residue digestates (Agri_1, 2 and 3). Similar observations on bovine manure and energy crops digestate
373 (BD) were made by Grigatti et al. (2019). Then the biowaste and agro-food industries digestates (BW_1,
374 Centr_1 and 2) had also high labile-P. The FFMSW samples showed intermediate P accessibility. The
375 sludge samples were characterized by a high NaOH extractable P, related to metal-bounded P. Indeed,
376 this result was consistent with both Al and Fe content (≈ 7 and ≈ 37 g kg⁻¹). Li et al. (2018), showed
377 mainly NaOH extractable Al, while Fe was NaOH soluble being also extracted by HCl in sewage sludge,
378 thus showing Fe-bounded P was partially occluded. Amongst the others samples, compost Sludge_2
379 showed important poorly available HCl-P, being very similar to FFMSW_2, these results were consistent
380 with the P fractionation of composts showed by Grigatti et al. (2015, 2017, and 2019).

381 Finally, HCA showed six groups (clustering not shown). Groups were ordered according to the chemical
382 availability level (i.e. Labile-P > NaOH-P > HCl-P) as follow: (i) Very high P accessibility related to high
383 H₂O-P fractions: digestates from liquid feedstock (no manure), biowastes and winery (BW_1, D1 and
384 D2). These samples were characterized by amorphous P and crystalline P (quartz and struvite); (ii) High
385 P accessibility associated with organic H₂O-P and NaHCO₃-P: digestates from liquid manure (BD and
386 Agri_2). These samples were characterized by crystalline P (struvite); (iii) Moderate P accessibility
387 (intermediary P speciation): digestates from organic fraction from municipal wastes digestates and
388 centralised digestates (FFMSW_1, FFMSW_2, Centr_1 and Centr_2). These samples were characterized
389 by an amorphous phase and mainly quartz and calcite as crystalline phases; (iv) Poor-P accessibility
390 associated with organic NaHCO₃-P and NaOH-P, associated with digestates from fibrous substrates as
391 cow manure with crops residues and wheat straw (Agri_1 and Agri_3). These samples were

392 characterized by a high amorphous phase; (v) Very poor P accessibility associated with inorganic NaOH-
393 P and low fraction of available P: digestate from solid phase of sludge (Sludge_1). This sample was
394 characterized by a crystalline P phase (mainly quartz and calcite); (vi) The poorest accessible P
395 associated with inorganic HCl-P was compost of sludge digestate (Sludge_2). This sample was
396 characterized by less crystalline P than Sludge_1 with calcite and quartz.
397 For some groups, the feedstock type seemed to have an impact on the P accessibility of digestates (solid
398 phase of sludge, liquid manure, liquid feedstocks, fibrous feedstock). Another observation was that the
399 amorphous and crystalline characteristics also seemed to be associated with some groups: fibrous
400 digestates were mainly composed of amorphous phase and contained organic P in NaHCO₃ and NaOH.
401 The labile P fractions had in common amorphous P and struvite as crystalline P. The most crystalline P-
402 rich fractions were found in the solid phase of sludge digestates before and after composting, containing
403 low available P and high sparingly soluble HCl-P.
404 The eight tested digestates represented a wide range of inherent characteristics and accessibility patterns
405 for both N and P. In this framework, the soil and plant test results can give a deeper insight to these
406 issues as discussed in the following section.

407 **3.2. Soil incubation and plant pot trials**

408 Table 4 shows the cumulative amount of biomass harvested in ryegrass plant pot tests. Any significant
409 differences between treatments for tissue and root (Kruskal-Wallis test $p=0.89$ and 0.23 respectively).
410 Nevertheless, it appears that poor biomass was obtained in Agri_2 treatment (pig manure digestate),
411 and in FFMSW_2 treatment (FFMSW digestate compost), close to the negative control. The best
412 results were obtained in Centr_1 and BW_1 (solid phase of a centralised digestate and biowaste
413 digestate). The total plant biomass (shoot+ root) was the highest (g pot^{-1}) in Centr_1 (4.11) \geq Sludge_2
414 (3.75) \geq BW_1 (3.72) \geq FFMSW_1 (3.70) \geq Ctrl+ (3.65) \geq Sludge_1 (3.48) \geq Agri_3 (3.38) \geq Centr_2
415 (3.23) \geq Agri__1 (3.18) \geq Agri_2 (3.02) \geq FFMSW_2 (2.93) \geq Ctrl- (2.90).

416 **3.2.1. Nitrogen fate**

417 The N mineralization data from soil incubation (Figure 3) showed the net cumulated mineral N (i.e.
418 $\text{NH}_4 + \text{NO}_3$ mass) during soil incubation (Figure 3a) and the net cumulated mineralization rate of
419 organic N (Figure 3b).

420 Concerning the available mineral N (N-min), BW_1, Centr_2, Sludge_1, Sludge_2, Agri_2 and
421 FFMSW_1 achieved the highest cumulated values after 84 days of incubation. On the contrary,
422 Centr_1, FFMSW_2, Agri_3 and Agri_1 performed poorly cumulated N-min. These latter were more
423 fibrous samples, with high C: N ratios.

424 The cumulated organic N mineralization rate was calculated (Figure 3b). Two groups of treatments
425 appeared and were classified in the same order than the cumulated N-min: (i) positive mineralization
426 rate associated with the Sludge_1, Centr_2, BW_1, Agri_2, Sludge_2 and FFMSW_1 treatments and
427 (ii) negative mineralization rate associated with Centr_1, FFMSW_2, Agri_1 and Agri_3. Sludge_1
428 showed the highest N mineralization rate (30%) suggesting that this digestate was rich in hydrolysable
429 proteins. Organic N from the liquid digestates Centr_2 and Agri_2 showed respectively 21% and 18%
430 of mineralized organic N, following Sludge_1 (30%). This result is consistent with Guilayn et al.
431 (2019) who reported that the highest organic N came from sludge digestate and pig-slurry digestate
432 group. Sludge_2 and FFMSW_1 performed lower N mineralization rates (11%). Similar results were
433 observed in liquid or solid digestates by Rigsby et al. (2013). They showed that the solid phase from
434 municipal solid wastes digestate (C: N ratio of 11) had negative N mineralization rate whatever the
435 soil composition used (sandy, silty or clay). On the contrary, Rigsby et al. (2013) showed that the
436 liquid digestates from slurry (C: N ratio of 4), had 16% to 40% N mineralization while food waste
437 digestate (C: N ratio of 14) reached 30% N mineralization.

438 The negative mineralization rates group was associated to an immobilization of mineral nitrogen by
439 the soil microorganisms during their growth (De la Fuente et al., 2013). This was related to the
440 increased microbial activity following the OW addition to the soil. Indeed, nitrogen is the main
441 limiting nutrient for plant growth, especially for a fast growing, highly demanding species such as
442 Italian ryegrass (Grigatti et al., 2011). These results are in agreement with Cavalli et al. (2017) which
443 reported immobilization for high C: N ratio anaerobic digestates. The authors showed the low C: N
444 ratio (5 to 7) associated to the raw digestate and its liquid phase (cattle slurry/mais silage) induced net

445 N mineralization ($\approx 30\%$). On the contrary, the cellulose- and volatile fatty acids-rich solid phase (C:
446 N ratio, 20) induced lower net N mineralization (9–16%). Indeed, negative correlations were found
447 between the N mineralization rate and C: N ratio ($r = -0.73$, $p = 0.029$) as observed by Morvan et al.
448 (2006) on animal manure wastes.

449 Considering the impact of process treatment of digestates, composting appeared to negatively affect N
450 mineralization. N mineralization rate from Sludge_2 (11%) was lower than Sludge_1 (30%) and
451 FFMSW_1 (11%) had highest mineralized values than FFMSW_2 (-2%). Phase separation impacted
452 also organic N mineralization as shown by Cavalli et al. (2017). Solid phase (Centr_1) reached
453 negative values of mineralization whereas Centr_2 reached 21% of mineralized N.

454

455 Plant growth experiments were affected by fertilizer treatment for N-ARF (Kruskal-Wallis, $p = 0.026$)
456 only for shoot plant tissues. Cumulated N recovery by plant tissues was plotted in the Figure 4. The
457 chemical treatment showed the greatest shoot N recovery (70%) with a total of 76% of N-ARF. N
458 uptake recovery was mainly observed in shoots (64% to 87% of the total recovery). Root N-ARF was
459 measured between 7% and 36% of the total N-ARF, except for Agri_1 and Agri_3 treatments where
460 negative to zero values were obtained.

461 Sludge_1 and Sludge_2 achieved the best N-ARF amongst the digestates treatments (16.5 and 15.1%).
462 These results were consistent with the Sludge_1 treatment yielding the highest N-min available for
463 plant growth. Centr_2 (13.7%), BW_1 (13.2%) and Centr_1 (11.6%) treatments showed intermediate
464 total N recovery. The FFMSW_1, FFMSW_2 treatments followed with 8.2% and 6.4% respectively.
465 Finally, a last group formed by Agri_1 and Agri_3 was observed with low N-ARF of 1.8% and 2.6%
466 respectively. In soil incubation tests, Agri_1 and 3 showed N immobilization. Accordingly to these
467 outcomes, the plant N-ARF was negative or close to 0 and close to the unfertilized soil treatment.

468 Considering the digestate treatments impact, composting (i.e. FFMSW_2 and Sludge_2) lowered the
469 fertilizing N value of its associated digestate (i.e. FFMSW_1 and Sludge_1 respectively). Phase
470 separation impacted also the N fertilizing potential as shown by Tambone et al. (2017). Centr_2
471 treatment induced higher N mineralization rates and N-ARF than Centr_1 treatment. According to N

472 speciation and characterization, the solid phase Centr_1 contained more fibers than the liquid phase
473 Centr_2.

474 PCA and HCA were performed to find correlations between the N availability data, digestate
475 characteristics, mineralized N percentages and N-ARF from shoots and roots as reported in Figure A.2
476 a (supplementary material). No significant correlation was observed between the total N content, the
477 mineralization rate and the N-ARF. However, a strong correlation was obtained between the C: N ratio
478 and N-ARF from shoots-N ($r=-0.82$, $p=0.004$) as in the mineralization N tests without plants. This was
479 described by a linear equation (Equation 8) based on the data of this study and validated by data from
480 digestates and composts studied in Grigatti et al. (2015). Similarly, Decoopman et al. (2017) found a
481 correlation between C: N ratio of agricultural digestates and plant N-ARF measured in field
482 experiments on cereals.

$$483 \text{Shoots}_N = -0.0085 \times \frac{C}{N} + 0.1782, r^2 = 0.6718 \quad \text{Equation 8}$$

484 The fiber component of digestates had a negative impact on mineralised N and N recovery by plant
485 tissues. Similarly, the fiber fraction PEOM of digestates was negatively correlated with cumulated
486 mineralized N (-0.58 , $p=0.08$) and shoots-N although to a lesser extent ($r=-0.58$, $p = 0.44$). Moreover,
487 cumulative mineralized N and shoots-N ARF were positively correlated ($r=0.72$, $p=0.02$) which was
488 consistent with the availability of N for plant growth. Concerning roots, there was a positive
489 correlation between roots N-ARF and nitrates content ($r=0.72$, $p=0.017$), SPOM_{NH₄} ($r= 0.61$,
490 $p=0.06$) whereas SPOM_{org} and roots_N ARF were negatively correlated ($r=-0.59$, $p=0.07$). A linear
491 equation (Equation 9) was found between Roots N-ARF and water extracted mineral N (i.e.
492 $N_{soluble_min} = NO_3^- + SPOM_{NH_4}$).

$$493 \text{Roots}_N = 5E^{-5} \times N_{solublemin} + 0.0138, r^2 = 0.5313 \quad \text{Equation 9}$$

494 According to Gunnarsson et al. (2010), plants respond to N availability with a different root/shoot
495 nutrient allocations and plant growth rate could be influenced by the ammonia/nitrates ratio in soil
496 solution due to the different N sources. Authors observed an increase in root biomass as a result of the
497 availability of a high amount of ammonia.

498 HCA revealed four clusters (Supplementary material Figure A.2.a) as follows: (i) Group 1: Agri 3
499 associated with fibrous digestate with high C: N (>25), high SEOM_N and PEOM_N and low shoots-
500 N ARF. This type of digestate is not suitable as N fertilizer; (ii) Group 2: FFMSW_2 and Agri_1
501 $15 < C/N < 13$, intermediary protein-like and fibrous substrate digestates with high organic SPOM_N
502 and PEOM_N for Agri_1 as compost FFMSW_2. They recovered very low roots N-ARF and
503 intermediate level of shoots N-ARF; (iii) Group 3: Centr_1, FFMSW_1 and BW_1 municipal solids
504 and biowastes digestates, with C: N ratios of 15 in average, high ammonium and nitrate levels in the
505 labile fraction and high levels of total N recovery; (iv) Group 4: The protein-like digestates (Sludge_1,
506 Centr_2, Agri_2) which have a poor C: N (<10), poor PEOM_N, high SPOM_Norg content and the
507 highest total N recovery. Sludge_2 was classified in the Group 4 because of its lower C: N ratio (9.7)
508 and its high N mineralization level.

509 C: N ratio is associated to the fibrous level of an OW and seemed to be discriminant enough to predict
510 N-ARF and organic N mineralization rate. Digestates with C: N ratios ≥ 15 were not suitable as N
511 fertilisers whereas digestates with lower C: N ratios had a high potential of N fertilizer.

512 Accessibility fractionation of N allowed a consistent digestate classification. Furthermore, interesting
513 correlation between roots-ARF N and water extractable nitrates and ammonia were found.

514 **3.2.2. Phosphorous fate**

515 The Olsen-P course during the soil incubation is shown by Figure 5a. The Olsen-P evolution in soil
516 depends on several phenomena: (i) the physico-chemical conditions of the soil can trap some weakly
517 bound P, (ii) the organic part of P can be mineralized and (iii) P can be taken up by soil
518 microorganisms for their growth.

519 The control soil had the lowest Olsen-P content throughout the incubation (12-14 mg kg soil⁻¹),
520 whereas the compared treatments exhibited different Olsen-P courses in time. All the tested samples
521 showed an available P depletion during the first two weeks. The chemical control (Ctrl⁺) performed
522 the fastest depletion. Indeed, the chemical P treatment (phosphate salt) can be rapidly fixed with Ca
523 components in calcareous soil (Albuquerque et al., 2012). In this context, the presence of organic

524 matter and the different P forms from digestates can have positive interactions with soil, performing
525 lower fixation and higher efficiency in comparison to chemical P sources (Albuquerque et al., 2012).
526 In some treatments, an Olsen-P increase appeared between 14 and 28 days (Agri_2, Centr_1, BW_1
527 and FFMSW_1) probably due to organic P mineralization before another decrease until 56 days. This
528 latter decrease led to a lower quantity of available P for plant growth. The RPE obtained was between
529 50 and 84%. The RPE of the Centr_2 treatment was the highest with 84% vs. the chemical P
530 treatment, followed by Sludge_2 (74%). FFMSW_1, Agri_2 and Agri_3 were the samples where the P
531 fixation was the highest (RPE of 60% in average). The other digestates were intermediate between the
532 two groups. FFMSW_1, Agri_2 and Agri_3 contained high fractions of water P.

533 The pot tests showed the treatments affected the plant P tissue (p-value = 0.021). In this context the
534 control soil performed the worst at the first cut (1.93 mg.pot⁻¹), showing very poor performance during
535 the plant pot test reaching 4.55 mg pot⁻¹ on average (Figure 5b and 5c). The shoot-P ARF is shown in
536 Figure 4a and b. P-ARF from Agri_2 and Agri_3 was negative from the beginning. This result was
537 consistent with the soil incubation observations. This can be linked with high fixation of P in soil as
538 suggested by Ahmad et al. (2018). In the second cut (day 56), the cumulative shoots P-ARF decreased
539 in all the treatments. Only FFMSW_1 and Centr_2 showed opposite outcomes. Then, between the
540 second and the third cut (day 56; 84), shoot-P ARF further increased. In the end the whole P-ARF (%)
541 was: Centr_1 (5.78)≈ FFMSW(5.31)≥BW_1 (4.35)>Centr_2(3.78)>Sludge_1 (2.72)≥Agri_1
542 (2.44)≥Sludge_2 (2)>FFMSW_2 (1.6)>Agri_2 (0.6)≈Agri_3 (0.5%).

543 FFMSW_2, Agri_2 and 3 showed lower shoots P-ARF than the chemical treatment (1.81%). That
544 means they were not suitable for P fertilization on calcareous soil.

545 The root-P content was unaffected by the treatment. However, the root P-ARF (%) was: Agri_1
546 (2.46)> Agri_3 (2.04)> FFMSW_1 (1.18) = Sludge_1 (1.17) = Sludge_2 (1.16)> Centr_1 (1.04)>
547 BW_1 (0.3)> Centr_2 (0.00)> FFMSW_2 (-0.08)>Agri_2 (-0.21). Shoots-P and roots-P recovery
548 potential were different depending on the treatment, except for Agri_2 and FFMSW_2 which had the
549 lowest ARF P recovery for both.

550 Briat et al. (2020) reported that availability of soil P (and K) for plants highly depends on the N
551 availability. They reported that P concentrations on shoots were correlated with N concentrations in
552 shoots. Indeed, a significant correlation was observed in this study between total N-ARF and total P-
553 ARF ($r = 0.8152$, $p = 0.0022$) with a linear relationship ($ARF_N/ARF_P = 7.7535$, $r^2 = 0.6626$) thus
554 proving N and P recovery by plants were linked.

555 PCA and HCA analysis were performed on both shoots and roots P uptake and P speciation for the 8
556 digestates studied beside the three digestates from Grigatti et al. (2019), as shown by Figure A.2 b in
557 Supplementary Material. Six groups were found according HCA analysis. The results showed that the
558 P-ARF was classified not only according to the digestate's nature but also according to their P
559 accessibility. The groups found were: (i) group 1 : Sludge_2, compost of solid phase of sludge
560 digestate, HCl rich with an intermediate level of P recovered in shoots and roots; (ii) group 2 :
561 Sludge_1, solid phase of sludge digestate (inorganic $NaHCO_3$ and NaOH fractions rich), with an
562 intermediate level of P recovered in shoots and roots; (iii) groups 3-4 : Centr_1, FFMSW_1,
563 FFMSW_2, Centr_2, Agri_2 (intermediate to low total P-ARF); (iv) groups 5-7 : BW_1, D1, D2 and
564 BD (high total P-ARF and highest inorganic H_2O-P); (v) group 6 : Agri_1, Agri_3, fibrous digestates.
565 Agri_1 has high P total recovery in both shoots and roots as BD, but Agri_3 shows a high recovery
566 only in roots. It seems that the fibrous characteristic enhances P recovery above all in in plants roots
567 through the organic fraction of NaOH-P.

568 The groups obtained were similar to digestate typology groups, except for Agri_2 and BD which were
569 not in a same group. When doing statistical treatments on the shoots results and P speciation for the 8
570 digestates used in addition to the 3 digestates used by Grigatti et al. (2019), some correlations were
571 found. Water-P fraction was positively correlated with shoots ($r=0.49$, $p=0.09$). This result was also
572 observed by Grigatti et al. (2017) for composts. As reported by Ahmad et al., 2018, available P consists
573 in the exchangeable and soluble P corresponding to water and Na-bounded P fractions ($H_2O+ NaHCO_3$)
574 whereas occluded P consists into P bound with metals (Fe, Al) and Ca. However, a simple linear model
575 did not fit between inorganic H_2O-P fraction (H_2O-P_i) and shoots P-ARF. PLS model was used showing
576 that two main significant variables were needed to predict shoots P-ARF (Equation 10). H_2O-P_i fraction

577 impacted positively shoots P-ARF, as expected, whereas organic H₂O-P fraction (H₂O-P_o) had a negative
578 impact. Therefore, available form of P for shoots growth was associated to H₂O-P_i fraction, as expected.
579 H₂O-P_o fraction is accessible but has to be mineralized to be available.

$$580 \text{Shoots}_P = 0.1153 \times \text{H}_2\text{O P}_i - 0.2777 \times \text{H}_2\text{O P}_o + 0.0249, r^2=0.71 \quad \text{Equation 10}$$

581 No correlations were found between ARF results and TP or phosphates concentrations ($r=-0.12$,
582 $p=0.74$, $r=-0.26$, $p=0.46$ respectively) meaning that the TP concentration is not enough to predict P
583 uptake by plants.

584 Organic NaHCO₃-P fraction (NaHCO₃-P_o) was positively correlated with roots ($r=0.62$, $p=0.025$ with
585 D1, D2 and BD). Organic NaOH-P fraction (NaOH-P_o) was also positively correlated with roots
586 ($r=0.79$, $p=0.006$). A PLS regression model was found between roots P-ARF and inorganic and
587 organic P content in NaHCO₃-P and NaOH-P fractions (Equation 11).

$$588 \text{Roots}_P = 0.0955 \times \text{NaHCO}_3\text{P}_o + 0.0955 \times \text{NaOH P}_o - 0.0584 \times \text{NaHCO}_3\text{P}_i + 0.0128, r^2=0.8641$$

589 Equation 11

590 Negative impact of inorganic labile NaHCO₃ was found whereas organic P forms impacted positively
591 the roots P-ARF. As previously mentioned, phytate and others phosphates esters can be extracted in
592 the NaOH-P fraction (He et al., 2010). Roots can exude phosphatases able to hydrolyse phytate and
593 organic P forms able to be absorbed by roots (Lambers et al., 2006; Gerke et al., 2015).

594 Interestingly, roots and shoots P recoveries were correlated with different P fractions. Finally,
595 chemical nutrient equivalents were calculated for all the treatments. The obtained values were above
596 100% except for Agri_2 (35%) and Agri_1 if only shoots were considered. That means that all the
597 studied digestates (except from pig slurry) can substitute chemical P needs.

598 Similarly to N results, phase separation impacted the P fertilizing potential. The solid phase of
599 centralised digestate Centr_1 was more suitable as P fertilizer than Centr_2. Composting impacted
600 also the fertilizing value of the municipal waste digestates by lowering the P fertilizer potential relative
601 to its respective digestate. This trend was also showed by Sludge_1 (digestate) versus Sludge_2
602 (composted digestate). Knowledge of the availability of P and its effects makes possible to anticipate

603 fertilisation according to the soil composition (Albuquerque et al., 2012) and not only based on overall
604 P analysis. Indeed, this was the case of sludge digestates Sludge_1 and 2 which had the highest P
605 contents (same level of Centr_1) but their treatments obtained moderate P-ARF. From P results, first
606 guidelines can be given according to the digestate feedstock typology for the studied calcareous soil
607 and ryegrass. Pig manure digestate (Agri_2) seemed not suitable for P fertilization. Fibrous digestates
608 rich on wheat straw Agri_1 and 3 had very low P fertilizing potential whereas FFMSW_1 presented
609 higher potential as the solid phase Centr_1. The compost FFMSW_2 had also low P fertilizing
610 potential and the liquid phase Centr_2 was intermediate. Sludge 1 and 2 had intermediary results and
611 biowaste digestate BW_1 showed high N and P fertilizing potential.

612 **4. Conclusions**

613 This study focused on different typologies of digestates classified according to their process and to
614 their feedstock. In this context, both P and N speciations showed a wide accessibility range according
615 to feedstocks characteristics. The chemical accessibility indicators described the nutrient availability for
616 plants and allowed the digestates classification on N and P fertilizing potential basis. The N and P
617 speciation impacted the results from incubations with bare soil as well as the apparent coefficients of
618 the use of N and P by the plant for its growth. Depending on the tissue collected (shoot or root), the
619 speciation variables having a significant impact were different for P and N, for the type of calcareous
620 soil used. First models were found to predict P recovery in shoots and roots using P speciation.
621 Furthermore, C: N ratio value was significant and could be used for shoots N-ARF prediction whereas
622 mineral water extracted N could be used for roots N-ARF prediction. Thus, a more detailed knowledge
623 of the digestates would allow more adequate control of fertilization. Moreover, composting and phase
624 separation impacted the nutrient recovery and can be used as an actuator to propose different organic
625 fertilizers type. In terms of perspectives, field trials on contrasted soils qualities for crops with
626 contrasting nutrient needs should be carried out in order to offer a guide to fertilization by type of
627 digestate. Finally, N and P speciation studied could be used in dynamic models to improve soil and
628 plant model predictions for digestate use in agriculture.

629 **Acknowledgements**

630 This project is supported by the Agropolis Fondation under the reference ID 1502-302 through the
631 « Investissements d'avenir » program (Labex Agro:ANR-10-LABX-0001-01) and is part of the EU-
632 funded project AgreenskillsPlus. Authors acknowledge Antoine Haddon for his useful advices.

633 **References**

- 634 Ahmad, M., Ahmad, M., El-Naggar, A-H., Usman, A. D., Abduljabbar, A., Vithanage, M., Elfaki, J.,
635 Al-Faraj, A., Al-Wabel, M. I. (2018) Aging Effects of Organic and Inorganic Fertilizers on
636 Phosphorus Fractionation in a Calcareous Sandy Loam Soil, *Pedosphere*, 28(6), 873-883.
- 637 Albuquerque, J.A., de la Fuente, C., Campoy, M., Carrasco, L., Nájera, I., Baixauli, C., Caravaca, F.,
638 Roldán, A., Cegarra, J., Bernal, M.P. (2012). Agricultural use of digestate for horticultural crop
639 production and improvement of soil properties. *Eur. J. Agron.* 43, 119–128.
- 640 Bareha, Y., Girault, R., Jimenez, J., Trémier, A. (2018). Characterization and prediction of organic
641 nitrogen biodegradability during anaerobic digestion: A bioaccessibility approach. *Bioresource*
642 *Technology*, 263, 425-436.
- 643 Bareha, Y., Girault, R. Guezal, S., Chaker, J., Trémier, A. (2019) Modeling the fate of organic nitrogen
644 during anaerobic digestion: Development of a bioaccessibility based ADM1, *Water Research*,
645 154, 298-315.
- 646 Barlóg, P., Hlisnikovský, L. & Kunzová, E. (2019) Yield, content and nutrient uptake by winter wheat
647 and spring barley in response to applications of digestate, cattle slurry and NPK mineral
648 fertilizers, *Archives of Agronomy and Soil Science*.
- 649 de Boer, H. C. 2008. Co-digestion of Animal Slurry Can Increase Short-Term Nitrogen Recovery by
650 Crops. *J. Environ. Qual.* 37:1968-1973.
- 651 Briat, J.-F., Gojon, A., Plassard, C., Rouached, H., Lemaire, G. (2020) Reappraisal of the central role of
652 soil nutrient availability in nutrient management in light of recent advances in plant nutrition at
653 crop and molecular levels. *European Journal of Agronomy*, 116.

654 Cavalli, D., Corti, M., Baronchelli, D., Bechini, L., Marino Gallina, P. (2017) CO2 emissions and
655 mineral nitrogen dynamics following application to soil of undigested liquid cattle manure and
656 digestates. *Geoderma*, 308, 26-35.

657 Decoopman, B., Houot, S., Germain, M. Hanocq, D., Airiaud, A., Lejare, L., Lerouc, C. (2017) Valeur
658 azote des digestats de méthanisation. *Rencontres COMIFER-GEMAS*.

659 Dou, Z., Toth, J.D., Galligan, D.T., Ramberg Jr, C.F., Ferguson, J.D.: Laboratory procedures for
660 characterizing manure phosphorus. *J. Environ. Qual.* 29, 508–514 (2000).

661 EU, 1991. European Commission Directive of the Council of December 12, 1991 Concerning
662 the Protection of Waters Against Pollution Caused by Nitrates from Agricultural Sources
663 (91/676/EEC) European Commission, Brussels (1991), 1-8.

664 EU Fertilisers Regulation COM (2016) 157 final 2016 / 00084 (COD) Proposal for a Regulation on the
665 making available on the market of CE marked fertilising products and amending Regulations
666 (EC) No 1069/2009 and (EC) No 1107/2009

667 de la Fuente, C., Albuquerque, J. C., Bernal, M. (2013). Soil C and N mineralisation and agricultural
668 value of the products of an anaerobic digestion system. *Biology and Fertility of Soils.* 49. 313-
669 322.

670 Gerke, J. (2015) Phytate (Inositol Hexakisphosphate) in Soil and Phosphate Acquisition from Inositol
671 Phosphates by Higher Plants. A Review. *Plants* , 4, 253-266.

672 Gissén, C., Prade, T., Kreuger, E., Nges, I.A., Rosenqvist, H., Svensson, S.-E., Lantz, M., Mattsson,
673 J.E., Börjesson, P., Björnsson, L. (2014) Comparing energy crops for biogas production – yields,
674 energy input and costs in cultivation using digestate and mineral fertilization. *Biomass*
675 *Bioenergy*, 4, 199–2010

676 Grigatti, M., Boanini, E., Cavani, L., Ciavatta, C., Marzadori, C. (2015). Phosphorous in digestate-based
677 compost : chemical speciation and plant-availability. *Waste Biomass Valor*, 6, 481-493.

678 Grigatti, M., Boanini, E., Mancarella, S., Simoni, A., Centemero, M., Veeken, A.H. (2017). Phosphorous
679 extractability and ryegrass availability from bio-waste composts in a calcareous soil.
680 *Chemosphere*, 174, 722-731.

681 Grigatti, M., Boanini, E., Bolzonella, D., Sciubba, L., Mancarella, S., Ciavatta, C., Marzadori, C. (2019).
682 Organic wastes as alternative sources of phosphorus for plant nutrition in a calcareous soil.
683 Waste Management, 93, 34-46.

684 Gunnarsson, A., Bengtsson, F., Caspersen, S. (2010). Use efficiency of nitrogen from biodigested plant
685 material by ryegrass. Journal of Plant Nutrition and Soil Science, 173(1), 113-119.

686 Guilayn, F., Jimenez, J., Martel, J-L., Rouez, M., Crest, M., Patureau, D. (2019). Valorization of non-
687 agricultural digestates: a review for achieving added-value products. Waste Management , 86,
688 67-79.

689 He, Z., Zhang, H., Toor, G., Dou, Z., Honeycutt, C. W., Haggard, B., Reiter, M. (2010) Phosphorus
690 Distribution in Sequentially Extracted Fractions of Biosolids, Poultry Litter, and Granulated
691 Products, Soil Science, 175 (4), 154-161.

692 Hedley, M.J., Steward, J. W. B., Chauhan, B. S.(1982) Changes in inorganic and organic soil
693 phosphorous fraction induced by cultivation practises and by laboratory incubations. Soil Sci.
694 Soc. Am. J., 46, 970-976.

695 Jimenez, J., Aemig, Q., Doussiet, N., Steyer, J.-P., Houot, S., patureau, D. (2015). A new organic matter
696 fractionation methodology for organic wastes: Bioaccessibility and complexity characterization
697 for treatment optimization. Bioresource Technology, 194, 344-353.

698 Jimenez, J., Han, L., Steyer, J.-P., Houot, S., Patureau, D. (2017). Methane production and fertilizing
699 value of organic waste: organic matter characterization for a better prediction of valorization
700 pathways. Bioresource Technology, 241, 1012-1021.

701 Lambers, H., Shane, M.W, Cramer, M.D., Pearse, S.J, Veneklaas, E. J. (2006) Root Structure and
702 Functioning for Efficient Acquisition of Phosphorus: Matching Morphological and Physiological
703 Traits, Annals of Botany, 98(4), 693–713.

704 Lashermes, G., Nicolardot, B., Parnaudeau, V., Thuriès, L. , Chaussod, R. , Guillotin, M.L. , Linères,
705 M., Mary, B. , Metzger, L. , Morvan, T. , Tricaud, A. , Villette, C. , Houot, S. (2010) Typology
706 of exogenous organic matters based on chemical and biochemical composition to predict
707 potential nitrogen mineralization, Bioresource Technology, Volume 101(1), 2010, 157-164.

708 Li, M., Tang, Y., Lu, X.-Y., Zhang, Z., Cao, Y. (2018) Phosphorus speciation in sewage sludge and the
709 sludge-derived biochar by a combination of experimental methods and theoretical simulation.
710 Water Research, 140, 90-99,

711 Li, L., Pang, H., He, J., Zhang, J. (2019). Characterization of phosphorus species distribution in waste
712 activated sludge after anaerobic digestion and chemical precipitation with Fe³⁺ and Mg²⁺.
713 Chemical Engineering Journal, 373, 1279-1285.

714 Mazzini, S., Borgonovo, G., Scaglioni, L., Bedussi, F., D'Imporzano, G., Tambone, F., Adani, F. (2020)
715 Phosphorus speciation during anaerobic digestion and subsequent solid/liquid separation, Science
716 of The Total Environment, Volume 734.

717 Möller, K., Müller, T. (2012) Effects of anaerobic digestion on digestate nutrient availability and crop
718 growth: A review. Engineering in Life Sciences, 12 (3), 242-257.

719 Morvan, T., Nicolardot, B., Péan, L., 2006. Biochemical composition and kinetics of C and N
720 mineralization of animal wastes: a typological approach. Biology and Fertility of Soils, 42, 513-
721 522.

722 Rigby, H., Smith, S.R. (2013) Nitrogen availability and indirect measurements of greenhouse gas
723 emissions from aerobic and anaerobic biowaste digestates applied to agricultural soils (2013).
724 Waste Management, Volume 33(12), 2641-2652,

725 Schiemenz, K., & Eichler-Löbermann, B. (2010). Biomass ashes and their phosphorus fertilizing effect
726 on different crops. Nutrient cycling in agroecosystems, 87(3), 471-482.

727 Tambone, F., Orzi, V., D'Imporzano, G., Adani, F., 2017. Solid and liquid fractionation of
728 digestate: Mass balance, chemical characterization, and agronomic and environmental
729 value. Biores. Technol. 243, 1251-1256.

730 Tampio, E., Salo, T., Rintala, J. (2016). Agronomic characteristics of five different urban waste
731 digestates. Journal of environmental management, 169, 293-302.

732 Watanabe, F.S., Olsen, S.R.(1965) Test of an ascorbic acid method for determining phosphorus in water
733 and NaHCO₃ extracts from soils. Soil Sci. Soc. Am. Proc. 29, 677-678.

734 Table 1: Definition and origins of digestate samples

Sample Name	Type	Scale	Anaerobic Digestion conditions: type (dry or liquid), feed mode (batch or continuous) and temperature	Digester Hydraulic retention time	Post-treatment	Substrate	Reference
Agri_1	digestate	Operating scale (farmer)	Dry batch mesophilic	60 days	-	Cow manure	This study
Agri_2	digestate	Operating scale (farmer)	Liquid continuous mesophilic	60 days	-	Pig manure co-digested with energetic crop and vegetable residues	
Agri_3	digestate	Lab scale	Dry batch mesophilic	100 days	-	wheat straw silage	
Sludge_1	Solid phase from digestate	Operating scale (private agency)	Liquid continuous mesophilic	20 days	Press filter	wastewater treatment sludge	
Sludge_2	compost of solid digestate	Operating scale (private agency)	Liquid continuous mesophilic	20 days	Press filter and composting	digestate of wastewater treatment sludge (1/3) and green wastes (2/3)	
FFMSW_1	digestate	Operating scale (private agency)	Dry continuous thermophilic	20 days	-	Fermentable fraction from municipal solid waste (FFMW)	
FFMSW_2	compost of digestate	Operating scale (private agency)	Dry continuous thermophilic 20	20 days	Composting	96%FFMSW, 50% green waste, 14% agro-industrial wastes	
BW_1	digestate	Operating scale (governmental)	Liquid continuous mesophilic	60 days	-	Biowastes (60%) from supermarkets co-digested with agro-industrial wastes (28%) and crop residues (12%)	
Centr_1	Solid phase of digestate	Operating scale (governmental)	Liquid continuous mesophilic	45 days	screw press	Oil (20%), crop residues (10%), agro_industrial wastes (55%), sewage sludge (10%), biowaste (5%)	
Centr_2	Liquid phase of digestate	Operating scale (governmental)	Liquid continuous mesophilic	45 days	screw press		
D1	Digestate	Operating scale	Liquid continuous thermophilic	na	-	Wastewater treatment sludge	Grigatti et al. (2019)
D2	Digestate	Operating scale	Liquid continuous mesophilic	na	-	Wine sludge	
BD	digestate	Operating scale	Liquid continuous thermophilic	na	-	Bovine slurry and energy crops	

735

736

737 Table 2: Physico-chemical characteristics of the investigated digestates

Parameters	Units	Agri_1	Agri_2	Agri_3	Sludge_1	Sludge_2	FFMSW_1	FFMSW_2	BW_1	Centr_1	Centr_2	D1	D2	BD
TS	%	17.1%	4.4%	14%	22.4%	59.1%	19.7%	53.3%	24.9%	26.4%	6%	3.94%	3.09%	5.05%
VS	%TS	70.2%	70.1%	87.0%	51.7%	48.5%	48.7%	41.8%	79.0%	82.2%	60.0%	58.2%	59.4%	68.3%
TOC	$g.kg^{-1}$	382.90	404.71	454.83	283.35	258.01	279.30	232.55	438.64	438.17	320.53	344.2	397.8	515.0
COD	$g.kg^{-1}$	1104.00	1400.56	1235.50	679.00	726.00	712.09	536.00	1291.00	1245.00	1497.58	nd*	nd	Nd
TKN**	$g.kg^{-1}$	25.85	115.00	nd	40.36	26.40	22.20	13.61	29.79	23.33	75.67	nd	nd	nd
TKN***	$g.kg^{-1}$	27.98	44.53	17.72	43.06	26.61	17.78	15.39	30.89	28.62	45.47	47.8	44.9	43.0
C/N		13.68	3.52	25.67	6.58	9.70	15.71	15.11	14.20	15.31	7.05	7.2	8.9	12.0
NH₄⁺-N**	$g.kg^{-1}$	6.28	87.85	2.99	10.80	0.92	10.5	0.04	27.68	6.81	34.74	nd	nd	nd
P	$g.kg^{-1}$	5.36	10.37	4.00	20.44	16.15	4.21	4.23	10.79	6.93	17.98	7.1	18.4	6.2
K	$g.kg^{-1}$	21.22	27.41	12.98	2.15	4.90	11.49	8.22	7.25	4.86	16.10			
S	$g.kg^{-1}$	3.59	6.23	1.63	6.23	5.33	2.22	5.00	2.16	6.27	7.58		nd*	
Al	$g.kg^{-1}$	2.31	3.23	0.65	6.66	12.56	8.68	2.73	8.46	2.68	9.33			
Ca	$g.kg^{-1}$	18.53	23.08	13.44	69.08	41.25	37.05	29.72	42.31	17.56	27.08	10	37	11
Fe	$g.kg^{-1}$	1.58	2.81	0.94	42.60	37.48	5.79	5.06	7.89	11.54	12.07	1.9	8.6	1.0
Ca/P		0.29	0.27	0.24	2.08	2.32	1.38	1.19	0.73	1.67	0.67	1.4	2.0	1.7
Mg	$g.kg^{-1}$	5.49	6.28	1.56	3.52	3.72	3.24	4.29	3.47	1.98	5.13	2.8	11.6	5.2
References		This study										Grigatti et al. (2019)		

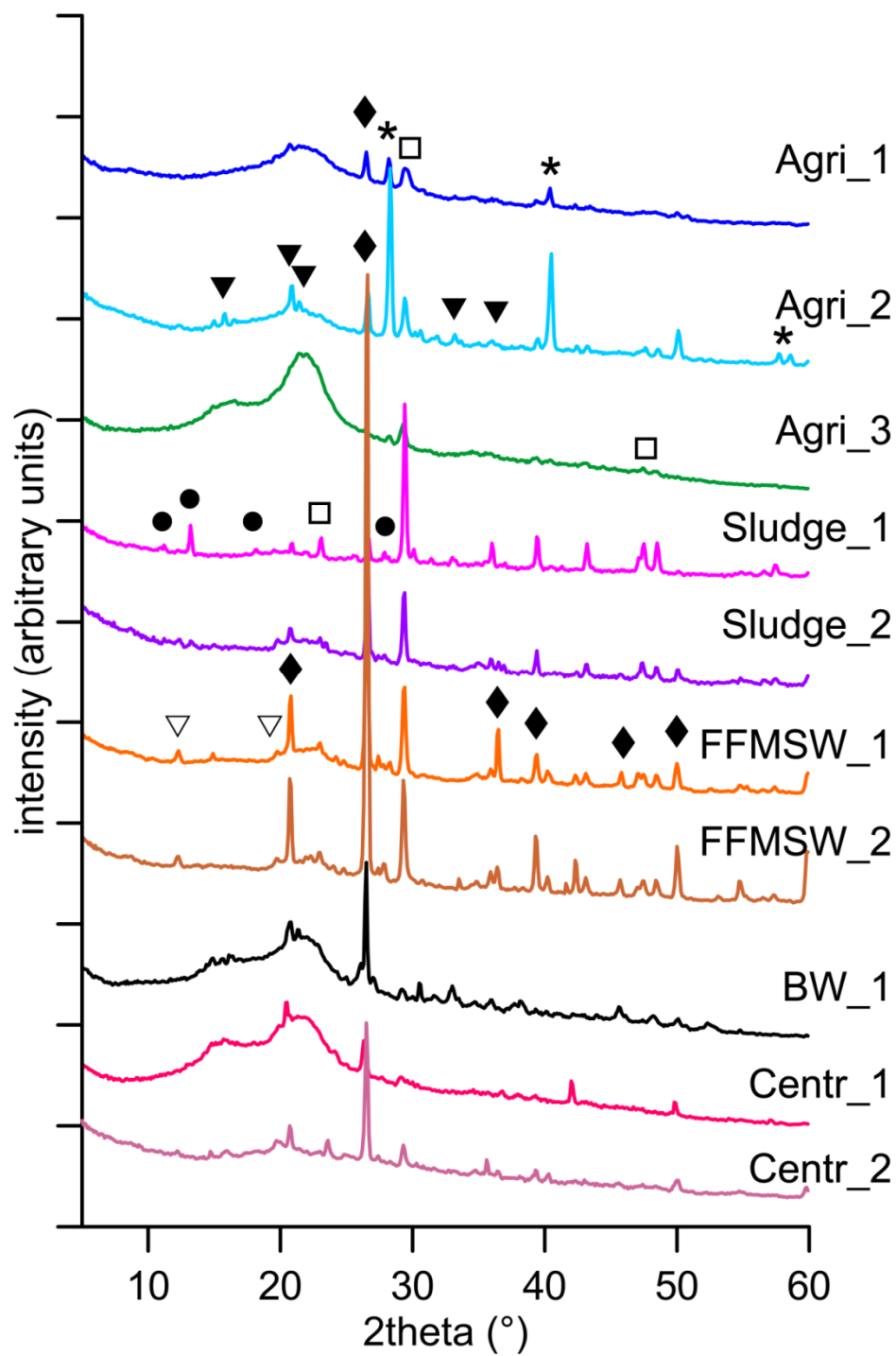
738 * nd : Not determined

739 ** Measured on raw samples

740 *** Measured on from freeze-dried samples

741 Table 3: Dry biomass (DW), total P uptake and N uptake in ryegrass shoots during three successive
 742 harvests (day 28-84) and roots at the final harvest (day 84)

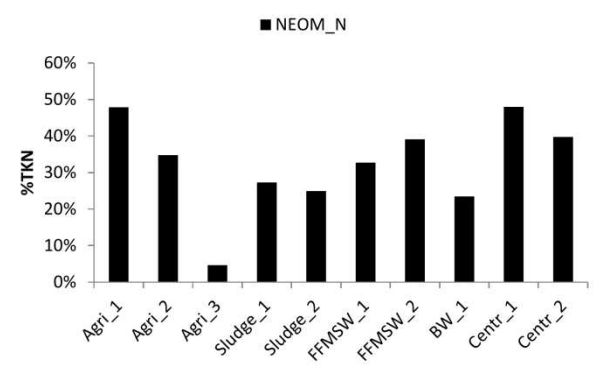
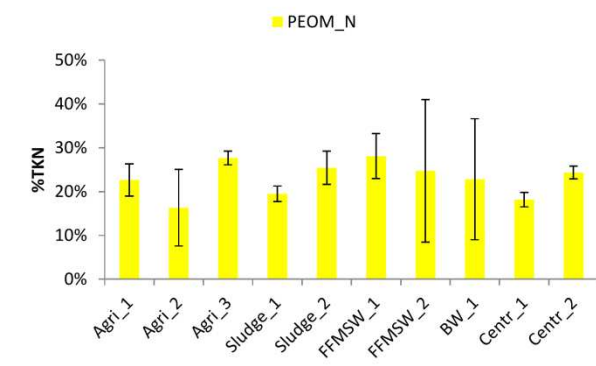
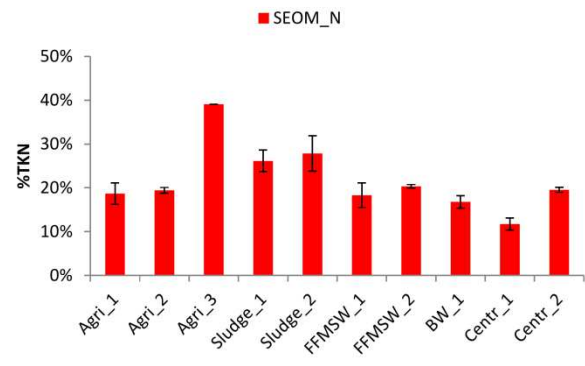
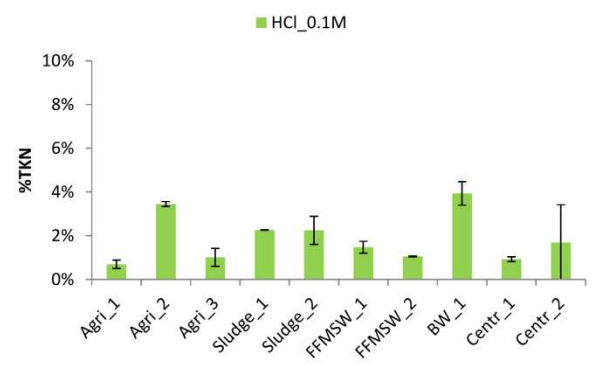
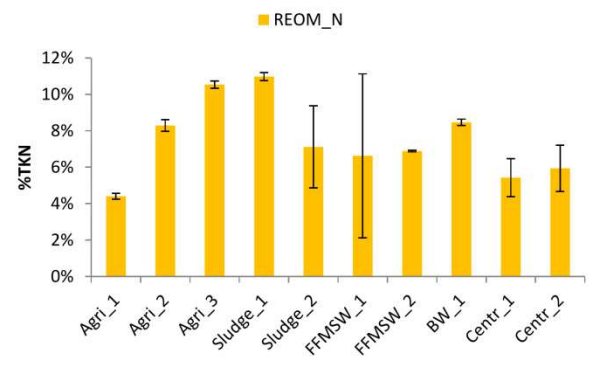
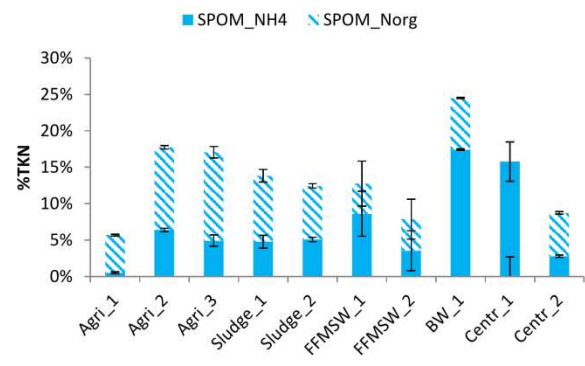
Treatment		Days after sowing						
		Shoots				Roots	Total	
		28	56	84	Mean	0-84	84	
<i>DW (g pot⁻¹)</i>								
	Ctrl-	0.87	0.53	0.25	0.55	1.65	1.25	2.90
	Ctrl+	1.00	0.70	0.39	0.70	2.09	1.56	3.65
1	Agri_1	0.88	0.50	0.29	0.56	1.67	1.51	3.18
2	Agri_2	0.86	0.58	0.35	0.60	1.79	1.23	3.02
3	Agri_3	0.84	0.44	0.27	0.52	1.56	1.82	3.38
4	Sludge_1	0.94	0.58	0.42	0.65	1.94	1.55	3.49
5	Sludge_2	0.94	0.57	0.37	0.63	1.88	1.87	3.75
6	FFMSW_1	0.85	0.58	0.36	0.60	1.79	1.91	3.70
7	FFMSW_2	0.88	0.47	0.26	0.54	1.61	1.32	2.93
8	BW_1	0.99	0.53	0.41	0.64	1.92	1.79	3.72
9	Centr_1	0.89	0.54	0.37	0.60	1.81	2.30	4.11
10	Centr_2	0.96	0.58	0.41	0.65	1.95	1.28	3.23
<i>P uptake (mg pot⁻¹)</i>								
	Ctrl-	1.93	1.60	1.02	1.52	4.55	2.25	6.80
	Ctrl+	2.17	1.48	1.43	1.70	5.09	2.24	7.33
1	Agri_1	2.41	1.14	1.61	1.72	5.16	2.87	8.03
2	Agri_2	1.81	1.15	1.76	1.58	4.73	2.19	6.92
3	Agri_3	1.87	1.07	1.76	1.57	4.70	2.86	7.56
4	Sludge_1	2.28	1.23	2.70	2.07	6.21	2.96	9.17
5	Sludge_2	2.29	1.53	2.32	2.05	6.14	3.18	9.32
6	FFMSW_1	2.05	1.76	2.41	2.07	6.21	2.62	8.84
7	FFMSW_2	2.65	1.13	1.35	1.71	5.13	2.22	7.35
8	BW_1	2.76	1.40	2.38	2.18	6.54	2.39	8.93
9	Centr_1	2.77	1.36	2.26	2.13	6.39	2.58	8.97
10	Centr_2	2.67	1.53	2.31	2.17	6.51	2.25	8.76
<i>N (mg pot⁻¹)</i>								
	Ctrl-	25.01	9.32	6.52	13.62	40.85	12.44	53.28
	Ctrl+	45.70	16.69	9.23	23.87	71.62	14.89	86.51
1	Agri_1	25.29	7.35	8.21	13.62	40.85	14.76	55.61
2	Agri_2	29.41	9.03	8.98	15.81	47.42	13.31	60.73
3	Agri_3	21.84	6.48	6.80	11.70	35.11	14.71	49.82
4	Sludge_1	36.91	10.51	12.39	19.94	59.81	15.13	74.93
5	Sludge_2	35.32	9.72	10.52	18.52	55.55	17.49	73.05
6	FFMSW_1	28.77	10.34	9.67	16.26	48.78	15.35	64.13
7	FFMSW_2	29.80	8.97	7.41	15.39	46.17	15.45	61.62
8	BW_1	32.03	9.97	11.88	17.96	53.88	16.51	70.39
9	Centr_1	30.74	9.28	10.00	16.67	50.02	18.45	68.47
10	Centr_2	34.63	10.39	12.16	19.06	57.18	14.04	71.22



743

744 Figure 1: X-ray diffraction of the digestates. The main peaks of different crystalline phases are

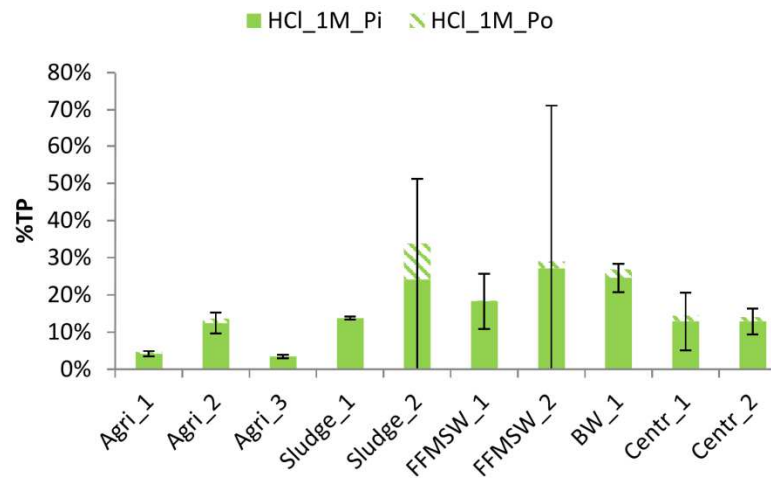
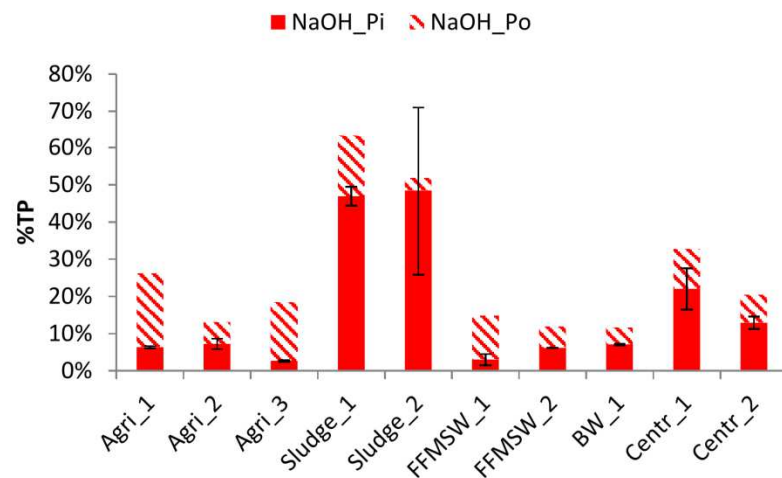
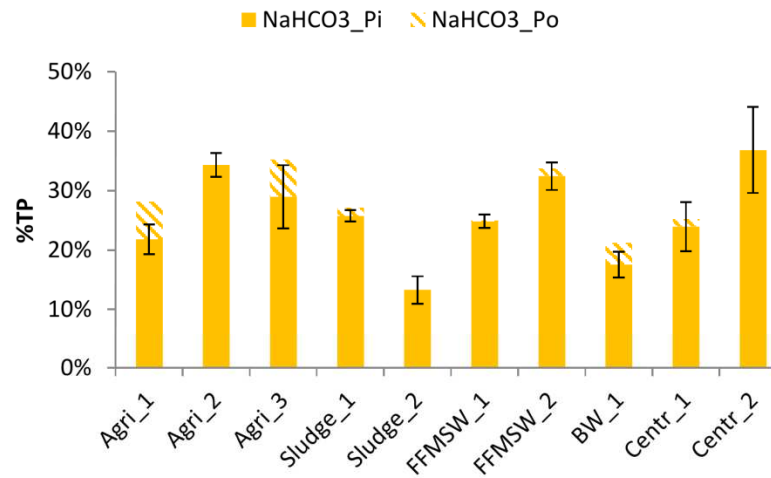
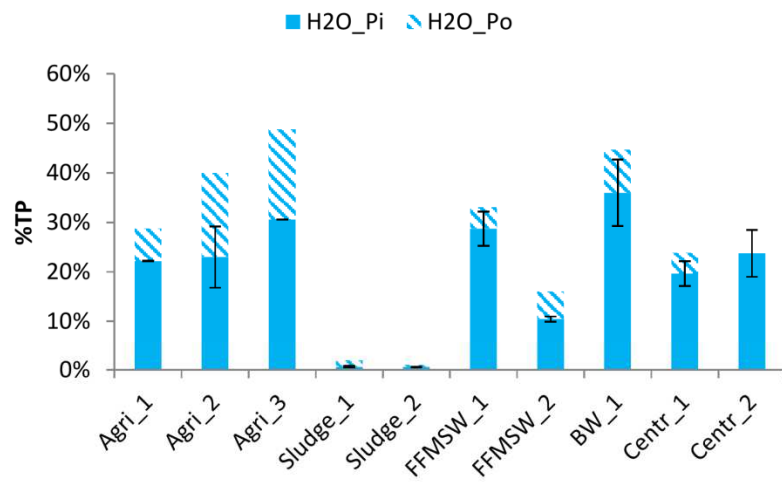
745 identified by symbols: ▼ struvite; ◆ quartz; □ calcite; ● vivanite; * sylvine; ▽ kaolinite.



746

747 (a)

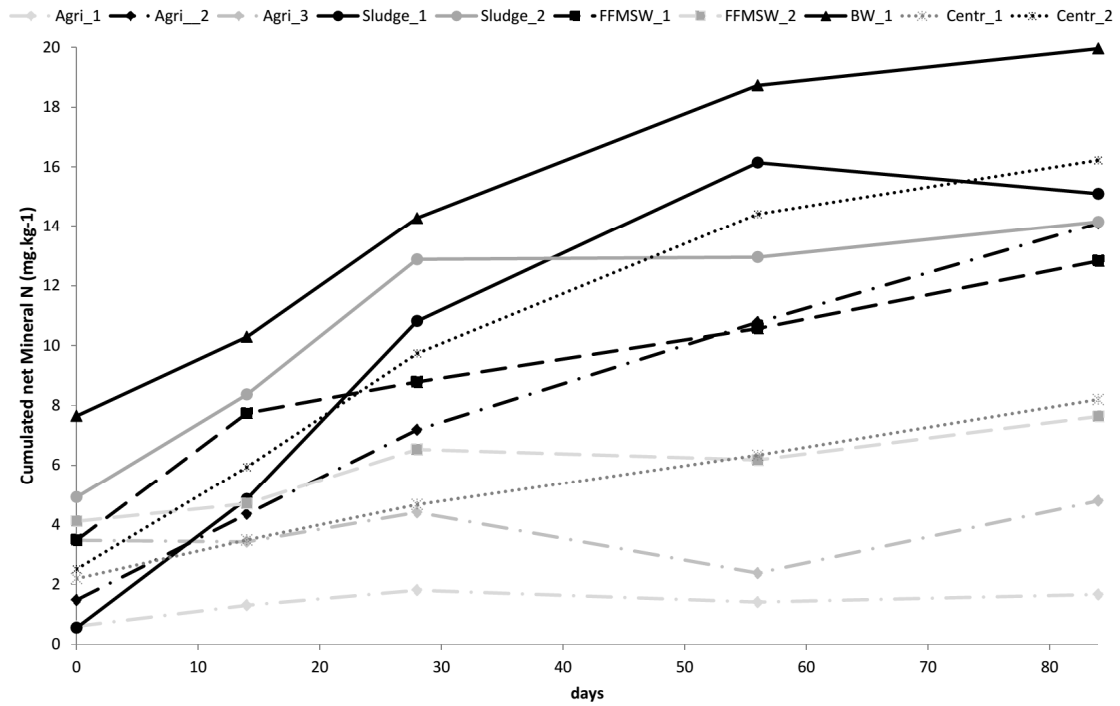
748



749

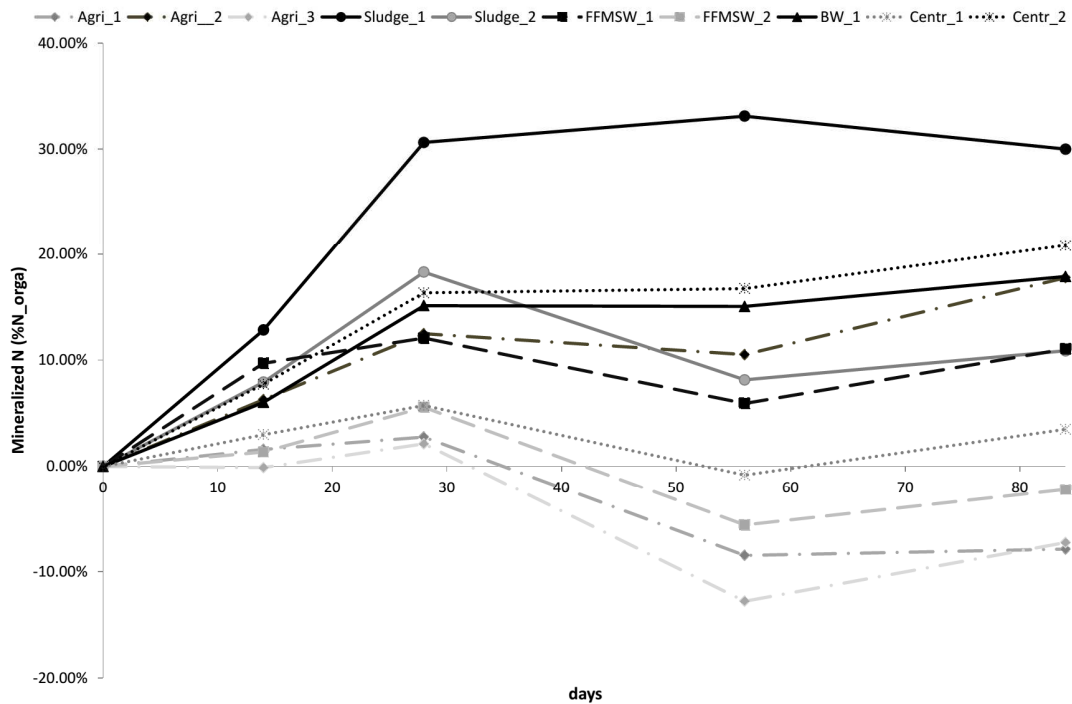
(b)

750 Figure 2: SCE fractions of TKN (a) and TP (b) obtained for all the digestates, according chemical accessibility. Error bars, SE (n=2)



751

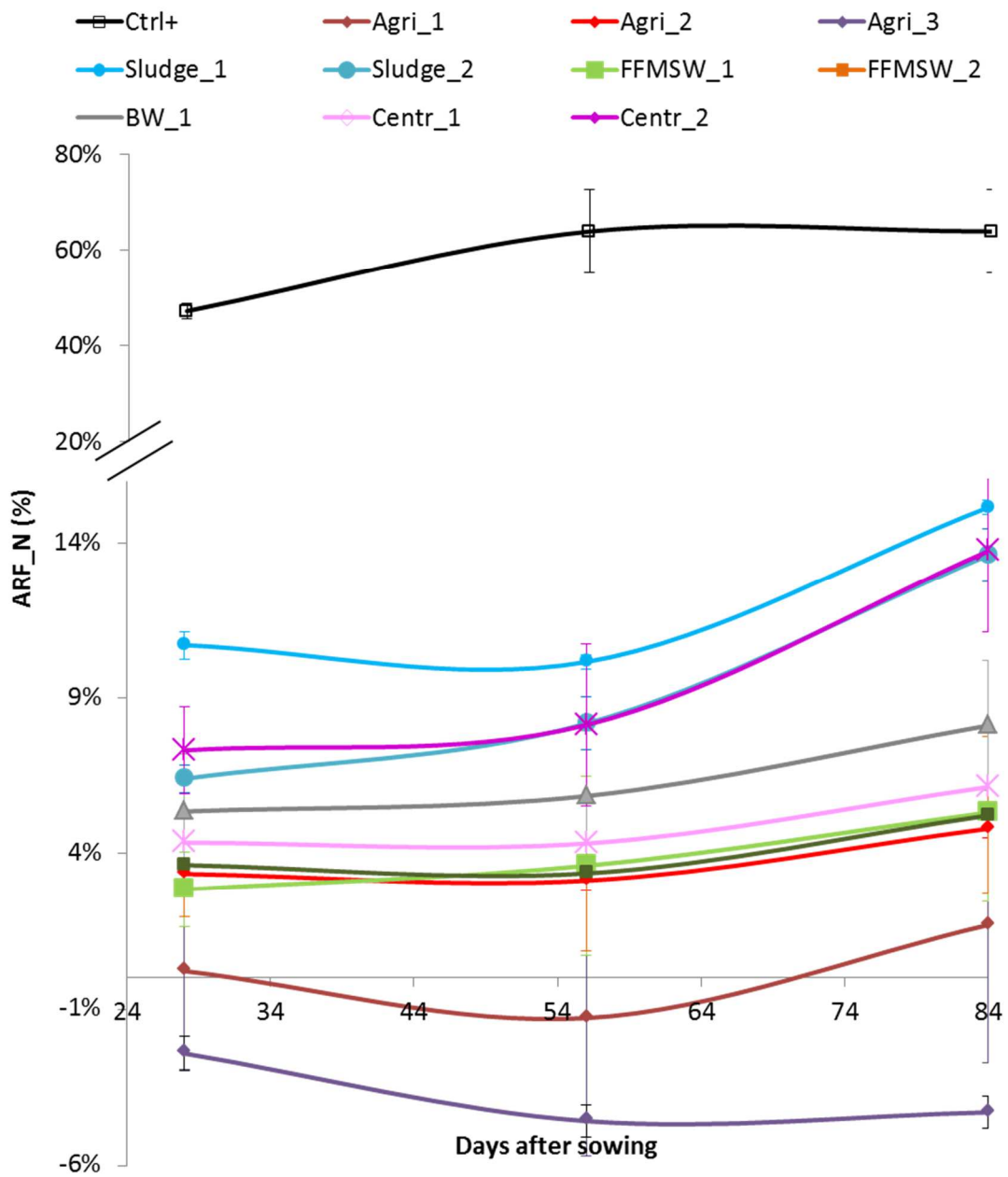
752 (a)



753

754 (b)

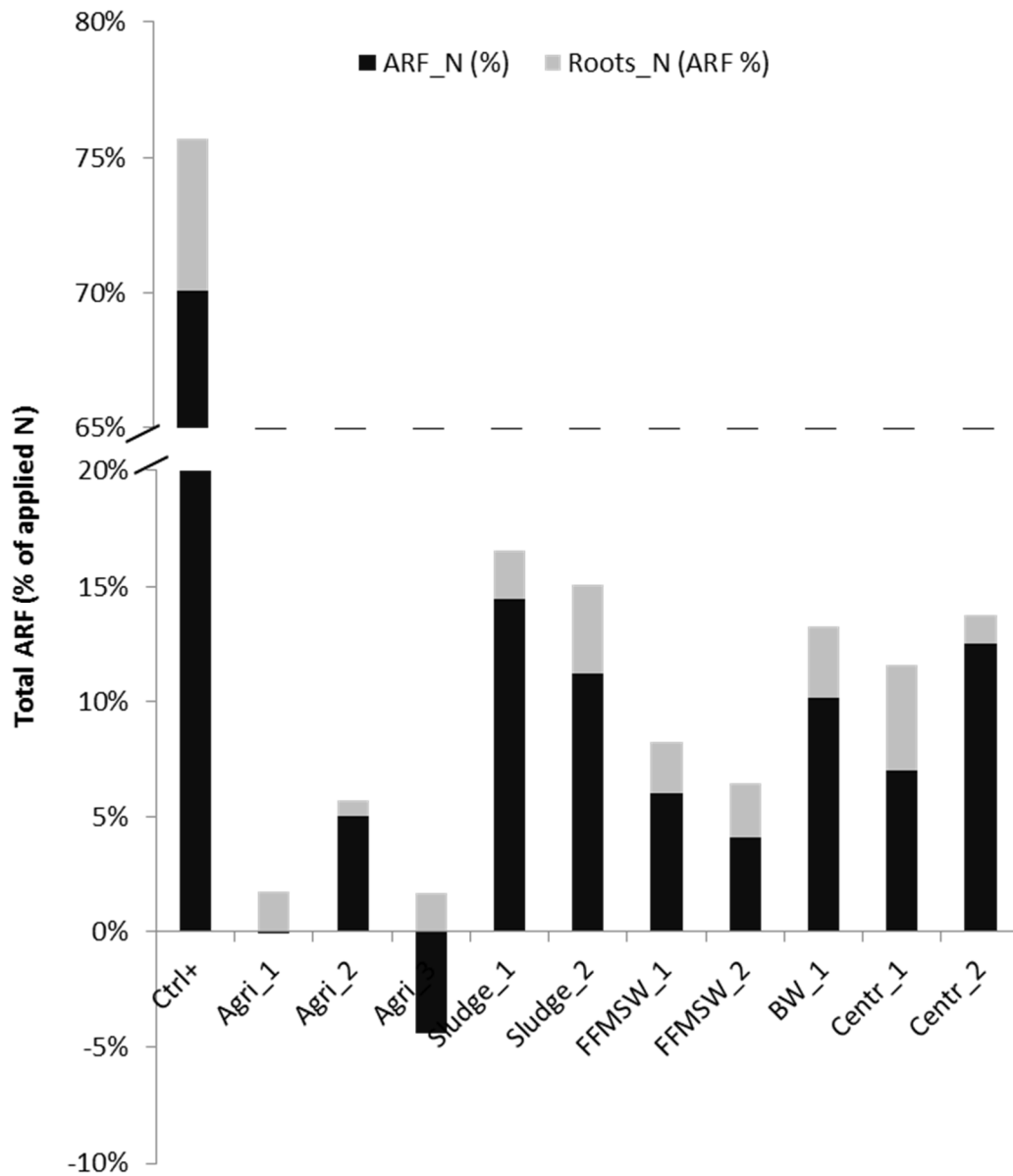
755 Figure 3: Cumulated mineral nitrogen concentration evolution (a) and cumulated mineralized organic
 756 nitrogen percentage (b) during soil incubation. Net values. *Black: high mineralized N group; Grey:*
 757 *low mineralized N group (circle+full line: sludge digestates, square+large dashes: FFMSW*
 758 *digestates, diamond+ dashes and dots line: Agrowastes digestates, triangle: biowaste digestate,*
 759 *cross+dotted line: centralised digestates)*



760

761 (a)

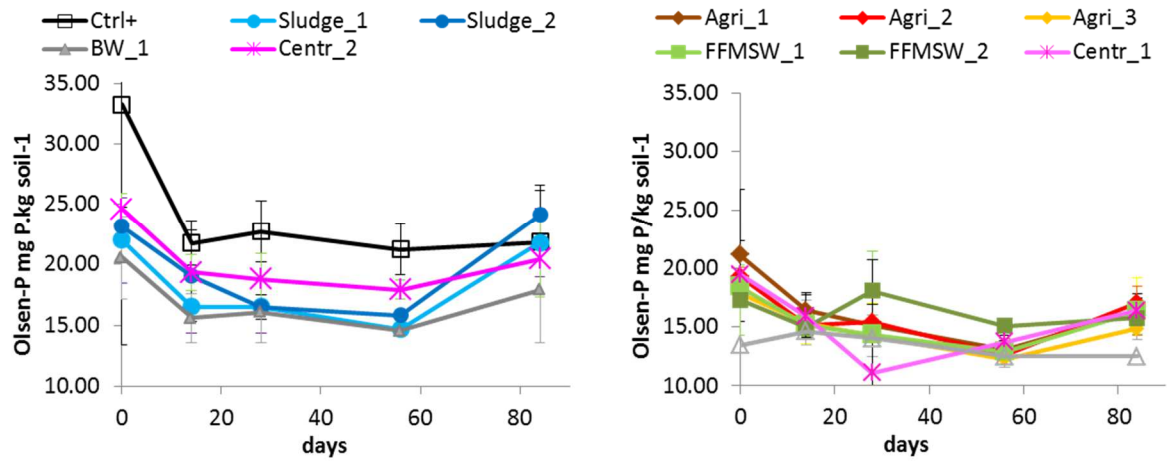
(a)



762

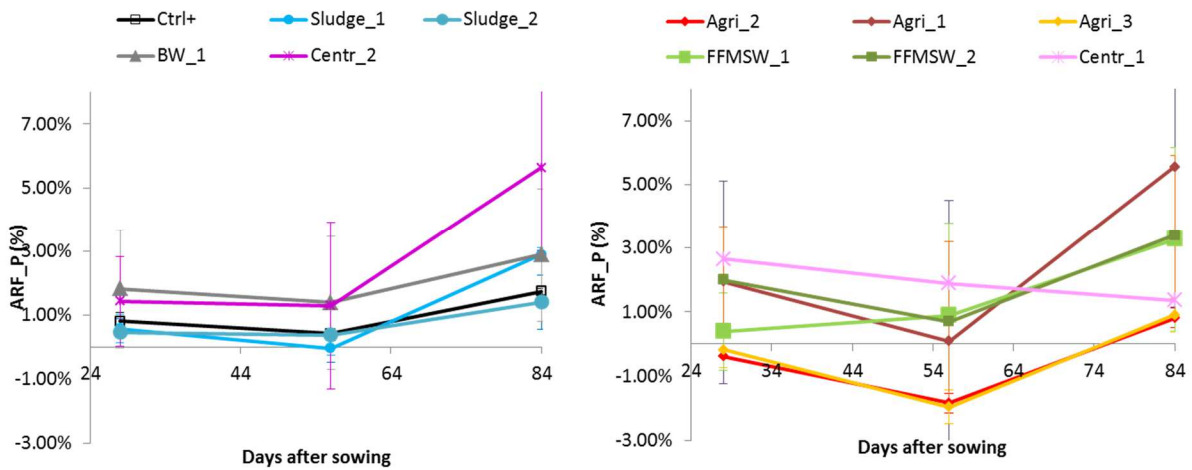
(b)

763 Figure 4: Nitrogen apparent recovery fraction (ARF) of ryegrass shoots (a) and in both shoots and
 764 roots (b) in three harvests during pot trial. Error bars, SE (n=3)



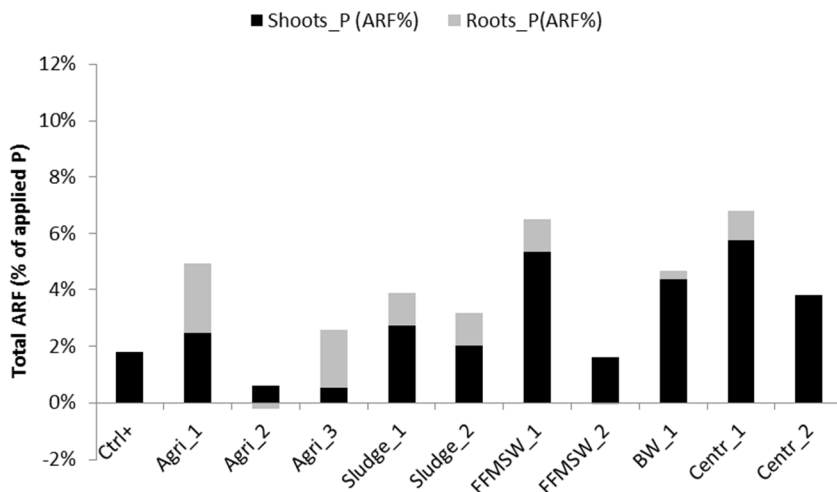
765

766 (a)



767

768 (b)



769

(c)

770 Figure 5: Olsen-P evolutions during the soil incubation of the tested digestates (a), cumulative
 771 phosphorous apparent recovery fraction (ARF) of ryegrass shoots (b) and in both shoots and roots (c)
 772 in three harvests during pot trial. Error bars, SE (n=3)